NATIONAL ADVISORY COMMITTEE FOR AERONAUTICS

REPORT No. 150

Copy #2 3

PRESSURE DISTRIBUTION OVER THICK AEROFOILS—MODEL TESTS

By F. H. NORTON and D. L. BACON

WASHINGTON
GOVERNMENT PRINTING OFFICE
1922

REPORT No. 150

PRESSURE DISTRIBUTION OVER THICK AEROFOILS—MODEL TESTS

By F. H. NORTON and D. L. BACON
Langley Memorial Aeronautical Laboratory

104374—22——1

1. FUNDAMENTAL AND DERIVED UNITS.

	Symbol.	Metric.		English.	
		Unit.	Symbol.	Unit.	Symbol.
Length	l	meter	m.	foot (or mile)	ft. (or mi.).
Time	t	second	sec.	second (or hour)	sec. (or hr.).
Force	F	weight of one kilogram	kg.	weight of one pound	lb.
Power	P	kg.m/sec		horsepower	HP
Speed		m/sec	m. p. s.	mi/hr	M. P. H.

2. GENERAL SYMBOLS, ETC.

Weight, $W = mg$.

Standard acceleration of gravity, $g = 9.806 m/sec.^2 = 32.172 ft/sec.^2$

Mass, $m = \frac{W}{g}$

Density (mass per unit volume), ρ

Standard density of dry air, 0.1247 (kg.-m.-sec.) at 15.6° C. and 760 mm. = 0.00237 (lb.-ft.-sec.)

Specific weight of "standard" air, $1.223 kg/m.^3 = 0.07635 lb/ft.^3$

Moment of inertia, mk^2 (indicate axis of the radius of gyration, k, by proper subscript).

Area, S; wing area, S_w, etc.

Span, b; chord length, c.

Aspect ratio = b/c

Length of body (from c. g. to elevator hinge), f.

Coefficient of viscosity, μ

3. AERODYNAMICAL SYMBOLS.

True air speed, V

Impact pressure, $q = \frac{1}{2} \rho V^2$

Lift, L; absolute coefficient $C_L = \frac{L}{qS}$

Drag, D; absolute coefficient $C_D = \frac{D}{qS}$

Cross wind force, C; absolute coefficient $C_C = \frac{C}{qS}$.

Resultant force, R

(Note that these coefficients are twice as large as the old coefficients L_c, D_c.)

Angle of setting of wings (relative to thrust line), i_w

Angle of setting of horizontal tail surface, i_t

Reynolds Number $= \rho \frac{Vl}{\mu}$, where l is a linear dimension.

e. g., for a model aerofoil 3 in. chord, 100 mi/hr., normal pressure, 0°C: 255,000 and at 15.6°C, 230,000;

or for a model of 10 cm. chord, 40 m/sec., corresponding numbers are 299,000 and 270,000.

Center of pressure coefficient (ratio of distance of c. p. from leading edge to chord length), C_p.

Angle of tail setting, $(i_t - i_w) = \beta$

Angle of attack, α

Angle of downwash, ϵ

REPORT No. 150.

PRESSURE DISTRIBUTION OVER THICK AEROFOILS—MODEL TESTS.

By F. H. Norton, and D. L. Bacon.

SUMMARY.

This investigation was undertaken by the National Advisory Committee for Aeronautics at the request of the Bureau of Construction and Repair of the Navy in order to study the distribution of loading over thick wings of various types. The loading on the wing was determined by taking the pressure at a number of holes on both the upper and lower surfaces of a model wing in the wind tunnel. The results from these tests show, first, that the distribution of pressure over a thick wing of uniform section is very little different from that over a thin wing; second, that wings tapering either in chord or thickness have the lateral center of pressure, as would be expected, slightly nearer the center of the wings; and, third, that wings tapering in plan form and with a section everywhere proportional to the center section may be considered to have a loading at any point which is proportional to the chord when compared to a wing with a similar constant section. These tests confirm the belief that wings tapering both in thickness and plan form are of considerable structural value because the lateral center of pressure is thereby moved toward the center of the span.

INTRODUCTION.

There have been previously made a considerable number of pressure distribution tests on aerofoils. As far as it is known, however, there have been no tests made upon wings of great thickness nor on wings of varying section. As the value of the cantilever wing is being more and more realized in modern machines, it has been found that the designers require more data than has previously been available on the loading along the ribs and along the spars of wings of this character.

In order to obtain data that could be used for any type of cantilever wing, the following set of 12 aerofoils have been tested:

1. Aerofoils of constant section and flat bottom but with varying height of upper camber.
2. Aerofoils of constant section and constant height of upper camber but with varying lower camber.
3. Sections thinned at the tip and having various degrees of lower cambers.
4. Wings with flat bottoms and proportional sections but tapering in plan form.

Below are given the more important references to pressure distribution over aerofoils:

Pressure distribution on the wings of a biplane of R. A. F. 15 section with raked tips—R. and M. No. 353, British Advisory Committee.

Distribution of pressure on the upper and lower wings of a biplane—R. and M. No. 355, British Advisory Committee.

Pressure distribution on model F. E. 9 wings—R. and M. No. 347, British Advisory Committee.

Investigation of the distribution of pressure over the center surface of an aerofoil—R. and M. No. 73, British Advisory Committee.

La Resistance De L'Air et L'Aviation—G. Eiffel.

Nouvelles Recherches sur la Resistance De L'Air et Aviation, G. Eiffel.
Essais D'Aerodynamique, troisieme serie, Armand de Gramont, duc de Guiche.
Etude des Pressious dynamiques sur les elements dune surface lamellaire—M. G. Lepère, Bulletin L'Institute Aerotechnique de L'Universite de Paris.
Essai D'Aerodynamique du plan, Armand de Gramont.
Essai D'Aerodynamique—Deuxieme serie Armand de Gramont.

APPARATUS AND METHODS.

As the expense of constructing metal aerofoils with air passages in them in the usual way (N. A. C. A. report No. 74) was exceedingly great, especially with wings tapering in section or plan form, it was found necessary to devise a new method of constructing aerofoils for pressure distribution in order to obtain a sufficient number of models with the allotted funds. After some experimenting it is found that models could be constructed of maple slightly under the required dimensions, with air passages grooved in the lower surface and pressure holes bored through the wings into these passages. A thin, hard paper was glued over the entire surface of the wing and given several coats of shellac, sealing the passages and bringing the model to the desired thickness. A section through a wing of this type is shown in Figure 1. This method gave a very smooth and satisfactorily accurate model.

The pressure holes on these wings were spaced as shown in Figure 2, using enough air passages to determine simultaneously the pressure on a set of holes along each chord on either the upper or lower surface. In making the test the holes on the outer row (either upper or lower) were pierced through the paper with a large needle, leaving a very clean hole with sharp edges. After the pressures had been taken along this row of holes for every angle of attack a thin sheet of paper was sealed tightly over the row with hot wax. The corresponding holes on the other surface were then pierced and the process repeated until the whole wing was tested. This method proved so expeditious that a wing could be completely tested at 45 points and for six angles of attack in one day by two men, including the preliminary plotting.

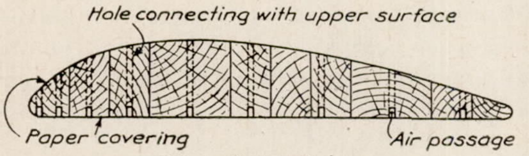

FIG. 1.—Section of wing.

The method of supporting the model and of taking off air leads to the manometer is shown in Figure 3. The head of a goosenecked spindle is screwed to the wing some distance from the center section and away from that end of the wing where the pressures are measured. The spindle is held in the chuck of an N. P. L. type balance and the angle of attack is adjusted by turning the balance head. Connection to the manometer is obtained by driving a set of tapered nipples into holes in the upper surface of the model, communicating with extensions of the air passages. Small rubber tubes slipped over these nipples communicate with the individual glass tubes of the multiple manometer.

Several tests intended to discover any interference between the spindle and air tubes and the nearest row of pressure orifices gave negative results and it is assumed that interference effects may be neglected.

The pressures from the wing were led through tubes to an inclined multiple manometer [1] for simultaneous readings of all the pressures (9) on one row. The reservoir of this manometer was connected to a static pressure head in the same section of the tunnel as the model. The pressures obtained were plotted directly as they were read from the gauge on the curve sheets, which saved a large amount of time in writing down figures and in replotting at a subsequent time. The areas between the curves for the upper and lower surfaces were planimetered, thus giving the normal force on the wings at that particular section. These areas were then plotted as ordinates along the span of the wing and the resulting curve gave the loading along the span. The area under this curve would represent the total load on the wing and the moment of this

[1] For description see N. A. C. A. technical note No. 36.

area about the center line of the wing corresponds to the bending moment at the root of the spars. The lateral position of the center of pressure on a half wing is determined by the quotient $\frac{\text{moment of area.}}{\text{area.}}$

THE SCOPE OF THE TESTS.

The first series of wings tested were of a constant section along the span 76.2×457 mm. (3×18 inches) and all had flat bottoms, the only difference between them being the height of the upper camber. The lift and drag coefficients for all of the wings tested in this report are given in National Advisory Committee for Aeronautics Report No. 152. It should be noted that all of the wings tested in this report have sections proportional to a master section for the upper surface and have either a flat lower surface or one proportional to a master lower camber. The second series consisted of wings with a concave or a convex lower camber but with the master section for the upper surface. The third series consisted of wings having the upper surface at the center the same as the master section but thinned towards the tips. The lower cambers were concave, flat, and convex. The fourth series consisted in wings having sections

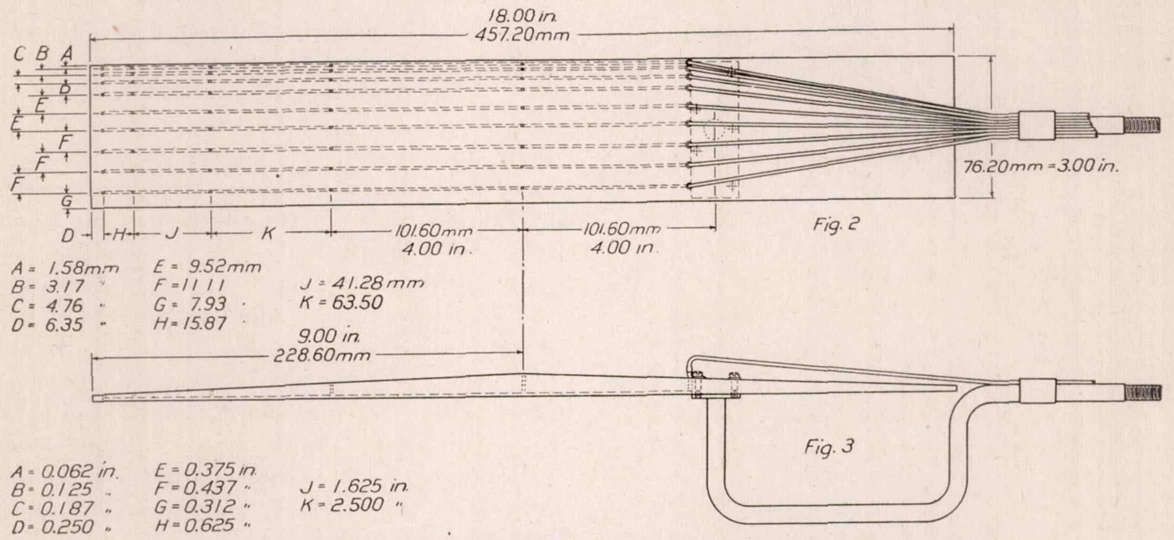

Showing location of pressure holes, tubes, and method of supporting model.

everywhere proportional to the master section and a mean aspect ratio of six, but tapering in plan form.

All of these wings were run at an air speed of 17.9 meters per second (40 miles per hour, 58.7 feet per second) but in most cases the wing was re-run either completely or in part at 26.8 meters per second (60 miles per hour, 88.0 feet per second) to see if any change in air flow was introduced by the higher speed. In the case of the thicker wings considerable difference was found between the two air speeds, especially around the angle of maximum lift, so that this feature was thought of enough interest to justify the plotting of the distribution of pressure for one of these wings (No. 68) at both speeds.

PRECISION.

The finished models were practically everywhere within 0.125 mm. of the given dimensions. Due to a slight warping of the tips of the thinned wings an extreme error of as much as 0.250 mm. or 0.375 mm. was introduced in some cases by this cause.

The accuracy of the pressure readings was limited by the fluctuations in air speed of the tunnel, but except around the angle of maximum lift the readings could be checked to within 2 per cent. The points on the pressure curves were carefully put in with a prick point and the curves have been drawn exactly through them in every case, but for the sake of clearness the points have been omitted in the figures.

The areas under the curve were planimetered with an accuracy of better than 1 per cent. An error somewhat larger than this was introduced, however, because of the incorrect drawing of the curve between the given point, especially where the pressure gradient is steep at the leading edge of the wing. In order to show the agreement between the normal force on the wing obtained by the integration of the pressures and that obtained by a force test of the same wing, using the wire balance, two curves are shown in Figure 4, and the agreement between them is considered to be quite satisfactory.

RESULTS.

As the loading on the wings is quite evident from the pressure curves (Figs. 9–35) included in this report, it is thought unnecessary to discuss the characteristics of the pressure at great length, so that only the more important points will be touched on. It should be noted, however, that the pressure curves plotted along the rib give valuable information as to the theory of design of thick wing sections and indicate more or less completely the reason for efficiency or inefficiency with any particular type of section.

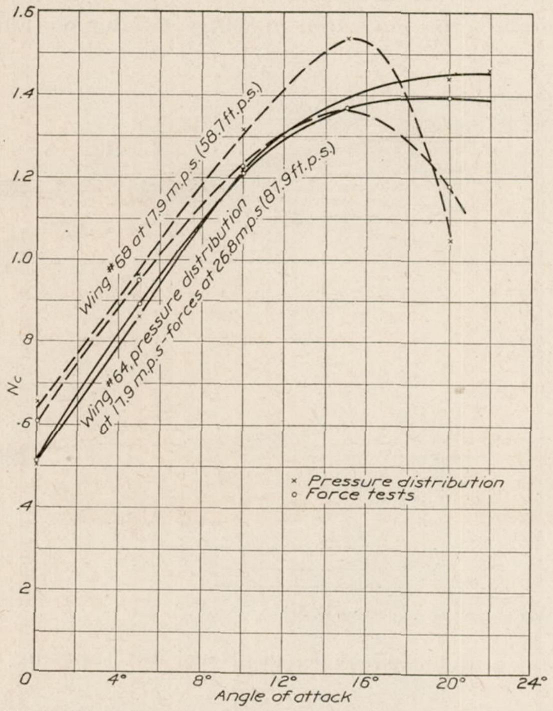

FIG. 4.—Normal pressure coefficient from integrated pressure and from force tests.

There is no distinguishing difference between the form of the pressure curve either along the chord or along the span as the thickness of the wing is increased with sections No. 69, No. 66, No. 64, and No. 68. For a given angle of attack, however, the thicker wings have a greater lift.

The phenomenon of burbling is shown up very clearly on most of these sections. It will be noted that as the angle of attack of the wing is increased the load on the wing increases up to a certain angle, at which point a certain section of the wing lying midway between tip and center begins to show a decrease in lift, while that at the center of the wing and the tips is still increasing. If the angle of attack is still further increased, the load at the tips still increases, but at the foregoing section and now also at the center of the wing it begins to decrease rapidly, with a consequence that the lateral center of pressure on the half wing moves rapidly outward. This outward movement of the center of pressure may amount to as much as 10 per cent of the semispan.

It has long been recognized from force tests on aerofoils that the region just beyond the point of maximum lift is very sensitive to changes in speed of test, and the reason for this is clearly brought out on wing No. 68, which is shown tested at 17.9 meters per second (58.7 feet per second) and again at 26.8 meters per second (87.9 feet per second). At the lower speed it is seen that the lift at the center of the wing begins to fall off rapidly beyond about 15°, whereas at the higher speed the lift keeps on increasing up to 20°, thus reaching a much higher total value. Below the burble point speed has no appreciable effect upon the pressure curve.

The effect of the speed of test on the distribution of load can perhaps be most clearly seen by turning to Figures 5, 6, and 7, which are photographs of two plaster models so constructed that the elevation of every point of the surface is proportional to the pressure coefficient on the corresponding point of the wing. Only one-half a wing is shown, with the center in the foreground. For the second model the test was run at 20° angle of attack and at 17.9 meters per second (58.7 feet per second), and it will be noticed that the load at the tip is considerably higher than at the center of wing, due to burbling. For the third model the conditions were exactly the same, excepting that the test was run at 26.8 meters per second (87.9 feet per second).

It will be noticed that an entire change in distribution has occurred, both along the ribs and along the spars. The frequent occurrence of such changes, always taking place near the angle of maximum lift, but not necessarily accompanied by any loss in lift, and caused merely by an increase in scale of test from $VL=1.36\frac{m^2}{sec.}$ to $VL=2.05\frac{m^2}{sec.}$, gives rise to the question whether the results obtained at or near the angle of maximum lift are of any value in the prediction of full-flight phenomena occurring at a scale from twenty-five to two hundred times as great. No apparatus was available to carry on laboratory tests at higher scale values than $VL=2.05\frac{m^2}{sec.}$ in order to investigate this possibility, but full flights about to be carried out will throw some light on this subject.

Wing No. 68 was run at angles of attack up to 90° in order to find out what the distribution of pressure was at these angles. Such high angles might be thought to be of little use in prac-

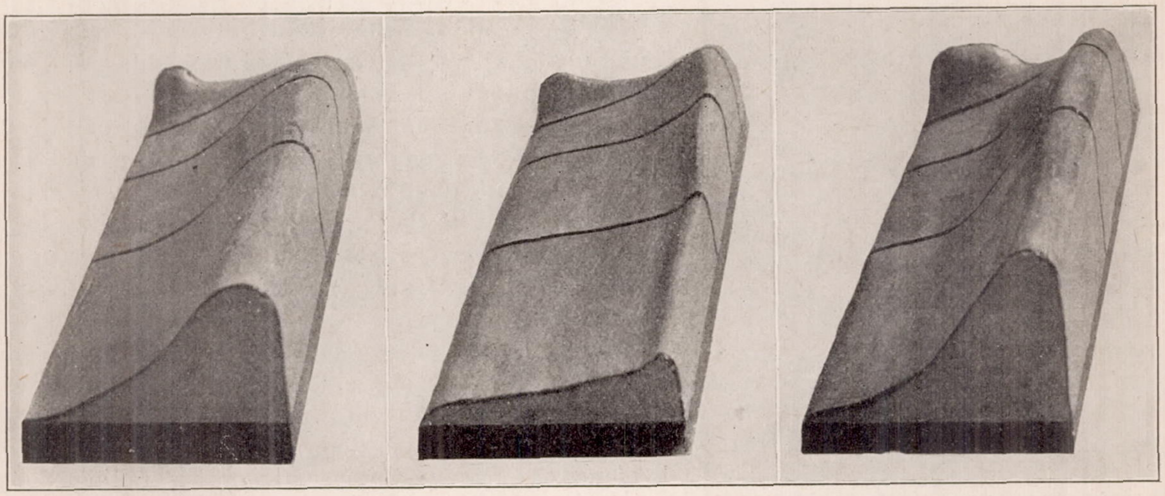

FIG. 5.—Pressure distribution over one-half of wing 68 at 15° angle of attack and at 17.9 m. p. s. (40 m. p. h.) (58.7 ft. p. s.).
The center of the wing (center of span) is in the foreground.

FIG. 6.—Pressure distribution over one-half of wing 68 at 20° angle of attack and at 17.9 m. p. s. (40 m. p. h.) (58.7 ft. p. s.).
The wing has now burbled, the lift decreasing markedly at the center.

FIG. 7.—Pressure distribution over one-half of wing 68 at 20° angle of attack and at 26.8 m. p. s. (60 m. p. h.) (87.9 ft. p. s.).
At this increased velocity the wing has not burbled and the lift coefficient is seen to be high.

tical aeronautics, but experiments that have been made on full-sized machines show that in a loop the angle of attack may rise to about 30°, while in a spin it commonly rises to over 60°. As the angle of attack approaches 90° the pressure on the lower surface is seen to become more and more uniform along the chord until it reaches a nearly constant value of the dynamic pressure. The suction on the upper surface approaches a semielliptical form, so that the center of pressure would then lie about halfway along the chord.

Another interesting feature shown by these tests is the very high peak at the trailing edge of the wing tip, which is perhaps most clearly shown in the photographs of the plaster models (Figs. 5, 6, and 7). This concentrated region of upload must have a very important influence upon the action of an aileron, especially one with a balanced portion at the tip, and may tend to explain the somewhat peculiar results that are at times obtained with ailerons balanced in this way. It has generally been considered that the loading along the span of a wing was of an elliptical form and this would be very closely true if this region of high pressure was neglected. At the higher angles of attack the distribution of load along the span is very nearly uniform, and for stress analysis and sand-load tests this uniform loading may be considered as very closely correct, although with a wing beyond the burble point the lateral center of pressure is more than halfway out toward the tip. In this connection it would seem probable that a wing tip having a negative rake would be of great help in reducing this local suction at the tip and giving a distribution of pressure more nearly elliptical.

In examining the curves of total pressure along the span it will be evident that at least at the higher angles of attack there is an oscillation in the curve. The first high peak occurs about one-tenth of the chord length from the wing tip, the second peak occurs at 0.8 chord length from the tip, while the third peak occurs at the center of the wing. It is thus seen that this oscillation increases uniformly in period as it recedes from the tip of the wing. The first peak of this oscillation occurring at the wing tip is due to the region of high suction at the trailing edge, which was discussed before. It seems quite evident that this oscillation in the curve of pressure is due to a vortex forming near the center of the wing and growing tighter as it approaches the tips, finally passing out at the trailing edge of the wing tip, leaving a region of high suction at its axis. This explanation is confirmed by the visual vortices which have been observed in the McCook Field wind tunnel and by Lanchester's vortex theory. At any rate, it is evident that we can not assume that the loading along the span approaches the elliptical form except at low angles of attack.

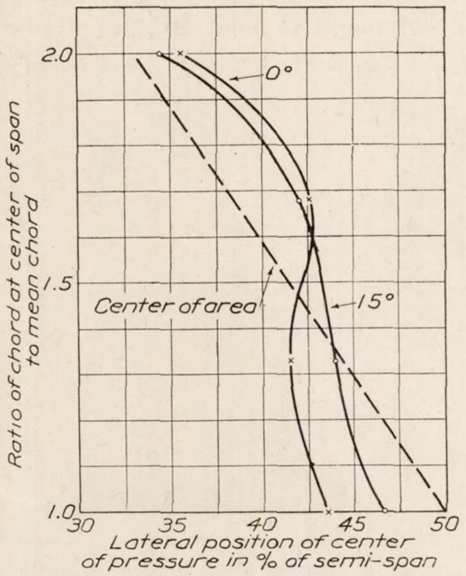

FIG. 8.—Effect of tapered plan form on lateral center of pressure. (Aspect ratio=6.)

In the second series of wings (sections No. 62, No. 64, and No. 65) where a lower camber was added to a constant upper section it is evident from the pressure curve that the pressure on the upper surface is practically unaffected by changes in the lower surface, and that the increased lift due to a concave lower camber is gained almost entirely by the increased pressure on the lower surface on the rear half of the chord. A change in the lower camber seems not to affect the loading along the span of the wing.

In the third series (sections No. 54, No. 56, and No. 58) where the wing is thinned at the tip it is evident that the load falls off rapidly toward the tip of the wing, as would be expected, and also that there is less evidence of a region of high suction at the trailing edge of the wing tip. Examination of the curves show, as in the preceding case, that the pressure on the upper surface is practically unaffected by changes in the lower camber. Also, as was shown before, the increased lift due to a concave lower camber is gained mainly by the increased pressure on the rear half of the lower surface. It is interesting to notice that these wings show even more markedly than the wings of uniform section that the burbling starts not at the center but about midway between tip and center. It may be concluded that thinning the wing tips, as has been done on section No. 66, moves the lateral center of pressure inward about 3.3 per cent of the semi-span, which means that for a given weight of airplane the bending moment at the root of the spars has been decreased by 8 per cent.

In the fourth series of wings (sections No. 64, No. 59, No. 60, and No. 72) where the plan form was tapered the pressures along each section have been plotted on a 76.4 mm. chord for convenience and have then been scaled to the true chord when plotting the curve of total pressure. It will be noticed that there is practically no difference in the pressure along any chord of this series of wings. As would be expected, the lateral center of pressure is moved inward as the taper of the wing is increased. In Figure 8 there is plotted a curve of center of pressure position against the amount of taper, and it will be seen that the center of pressure is moved in about 10 per cent of the semispan when the wing is tapered down to a point at the tip—as great a taper as is practicable. This C. P. movement decreases the bending moment by 25 per cent. If the wing is tapered both in thickness and in plan form, the center of pressure may be moved inward as much as 10 nor 15 per cent of the semispan more than for uniform section wings—a reduction in the bending moment on the spars of 20 to 30 per cent, which is well worth striving for.

GENERAL CONCLUSIONS.

This investigation shows that in designing ribs or spars for thick wings that the same manner of loading may be used as would be taken for thin wings. The distribution along the span is not elliptical and departs far from it at the higher angles of attack, due to a region of high suction at the trailing edge of the wing tip; so that in computing stresses or making sand load tests no more favorable condition than uniform loading along the span should be considered, and at angles above the burble point the conditions might be even more severe than this. Although experiments have not been made to show the fact conclusively, it seems possible that a negative rake on the wing tip will give a much more uniform loading to the wing and, as it is now well known, will give to the aileron a considerably higher efficiency. Tapering a wing either in plan form or in thickness decreases the load at the tip of the wing and thus moves the lateral center of pressure towards the center, so that from a structural point of view this fact is of considerable advantage. The bending moment at the root of cantilever spars may be reduced in this way by as much as 20 or 30 per cent.

104374—22——2

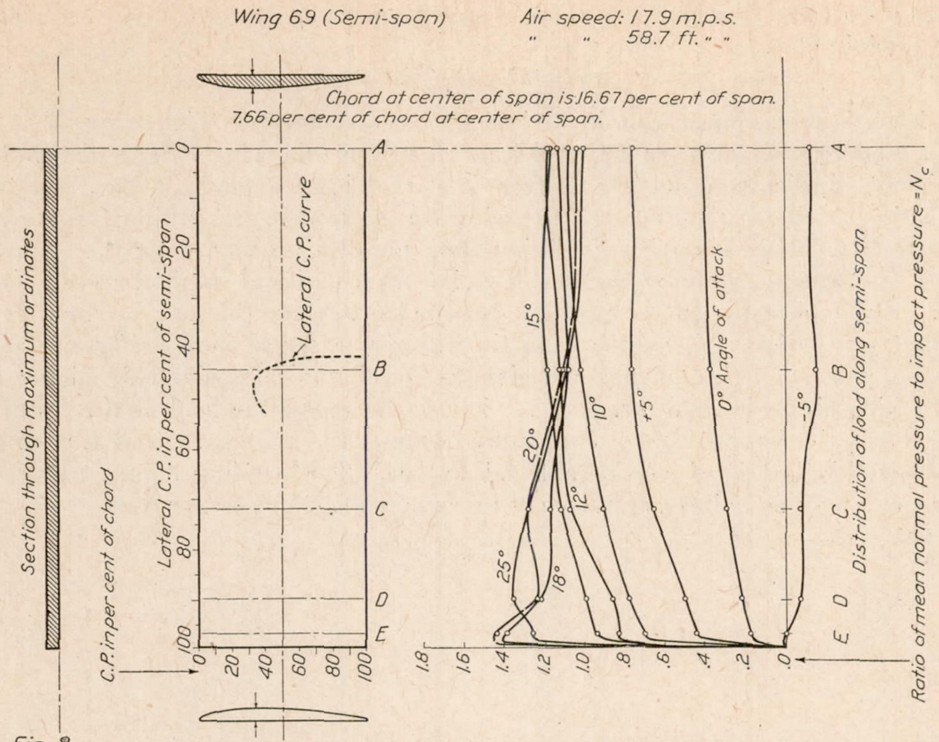
Wing 69 (Semi-span)
Air speed: 17.9 m.p.s.
" " 58.7 ft. " "
Chord at center of span is 16.67 per cent of span.
7.66 per cent of chord at center of span.
Section through maximum ordinates
C.P. in per cent of chord
Lateral C.P. in per cent of semi-span
Lateral C.P. curve
Angle of attack
Distribution of load along semi-span
Ratio of mean normal pressure to impact pressure = N_c
7.66 per cent of chord at tip.
Chord at tip is 16.67 per cent of span.

Fig. 9

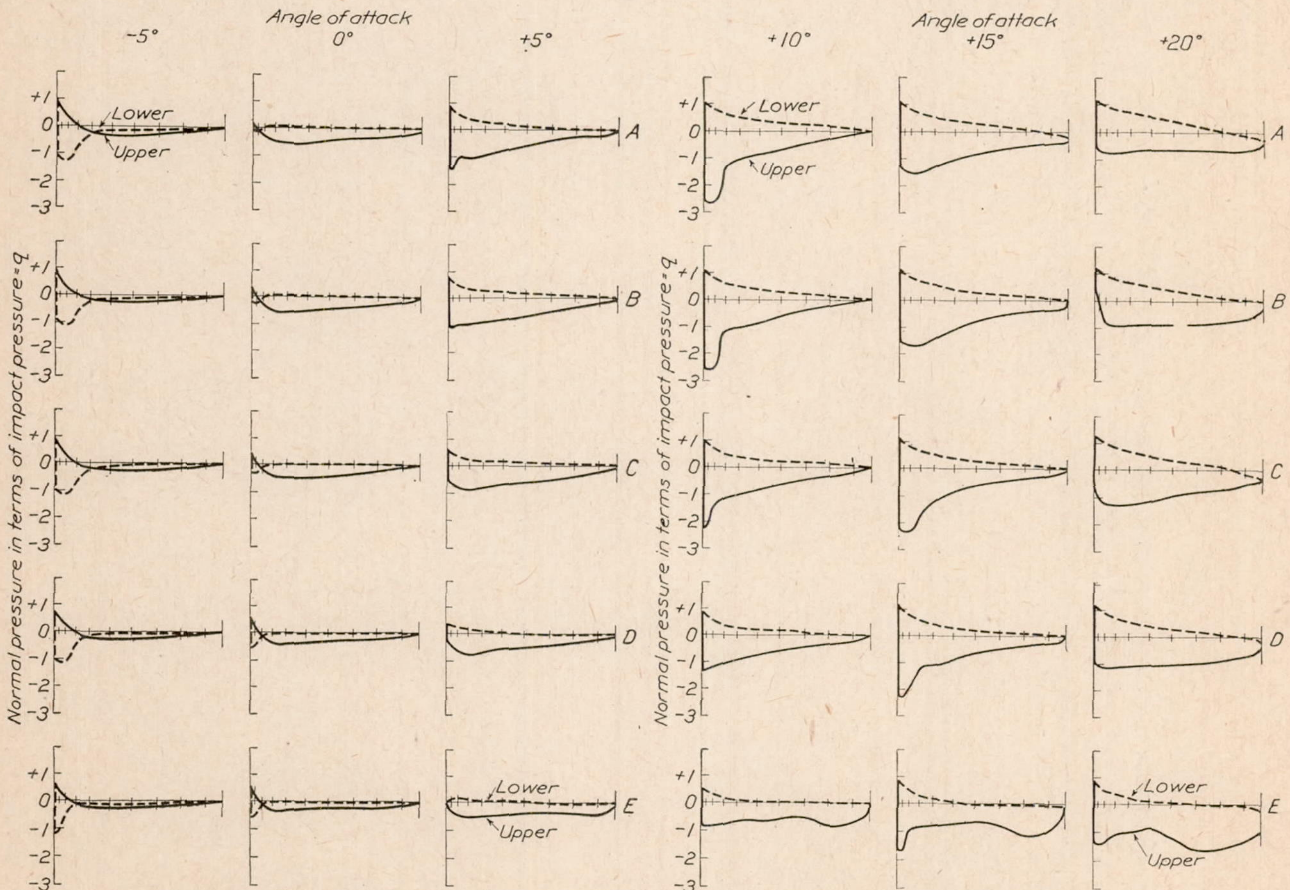
Angle of attack
-5° 0° +5° +10° +15° +20°
Lower
Upper
Normal pressure in terms of impact pressure = q
Distribution of load along chord

Fig. 10

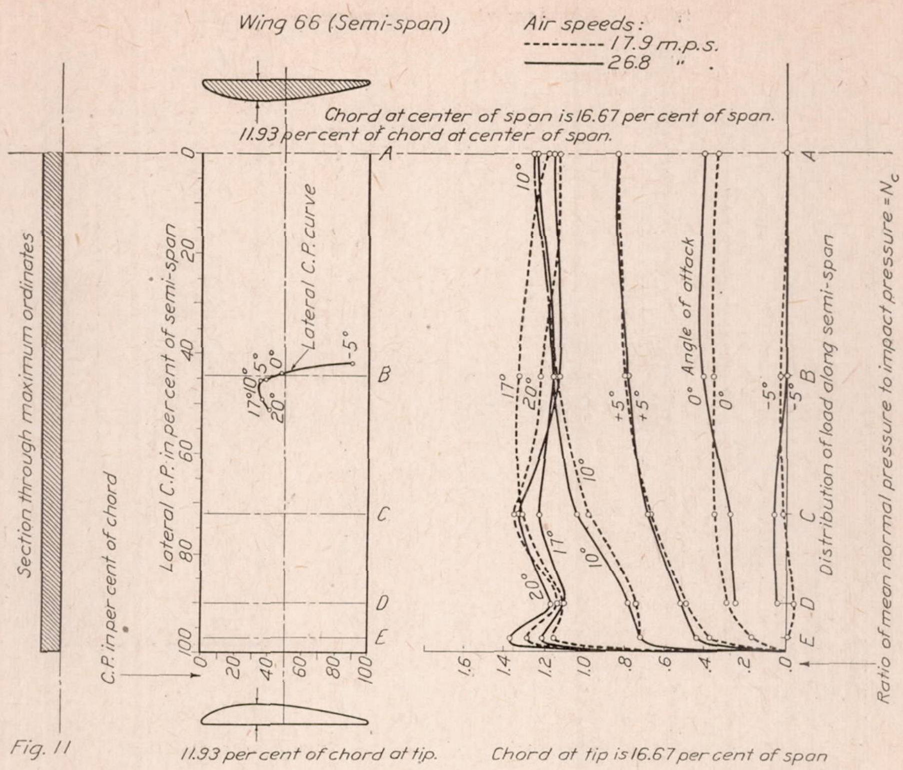

Fig. 11

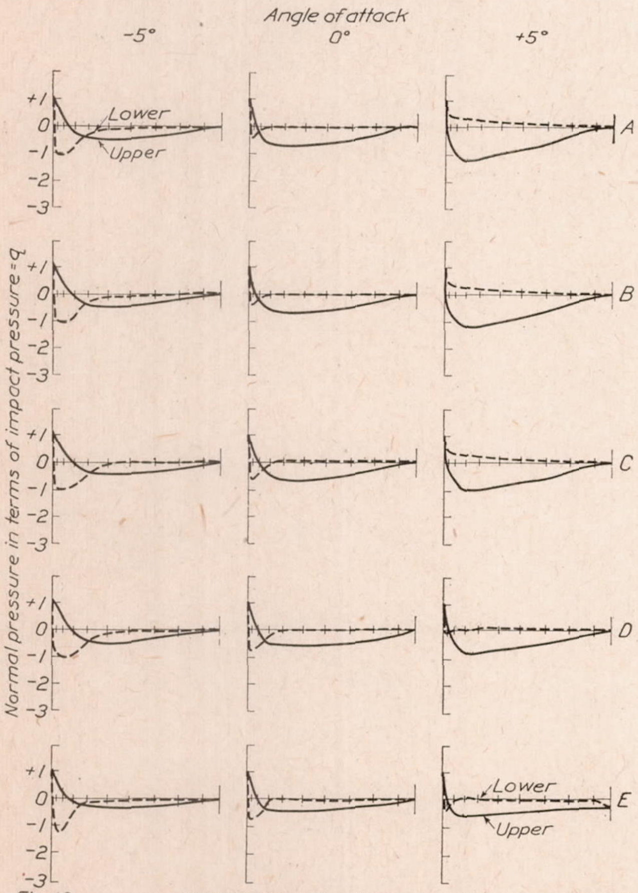

Fig. 12

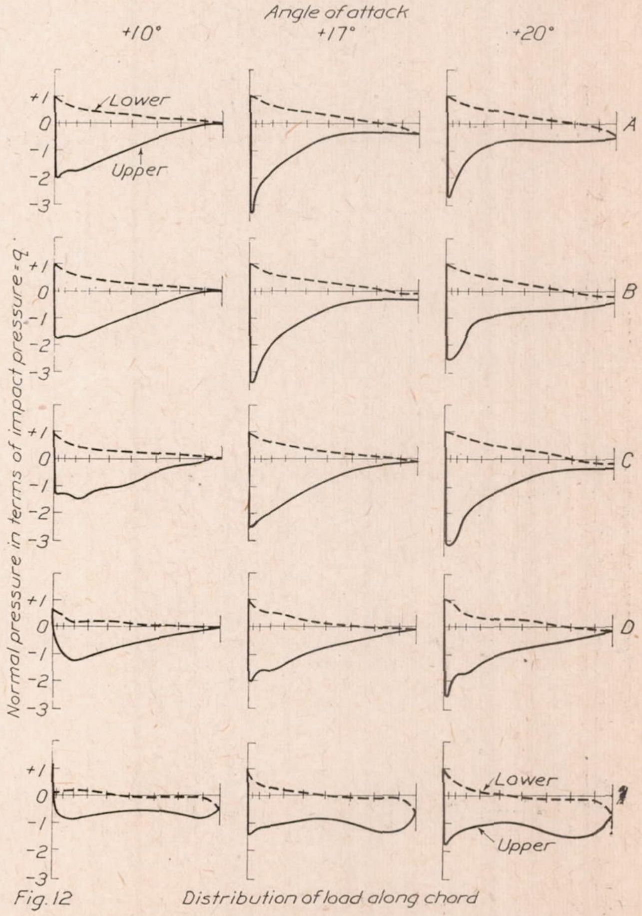

Fig. 12

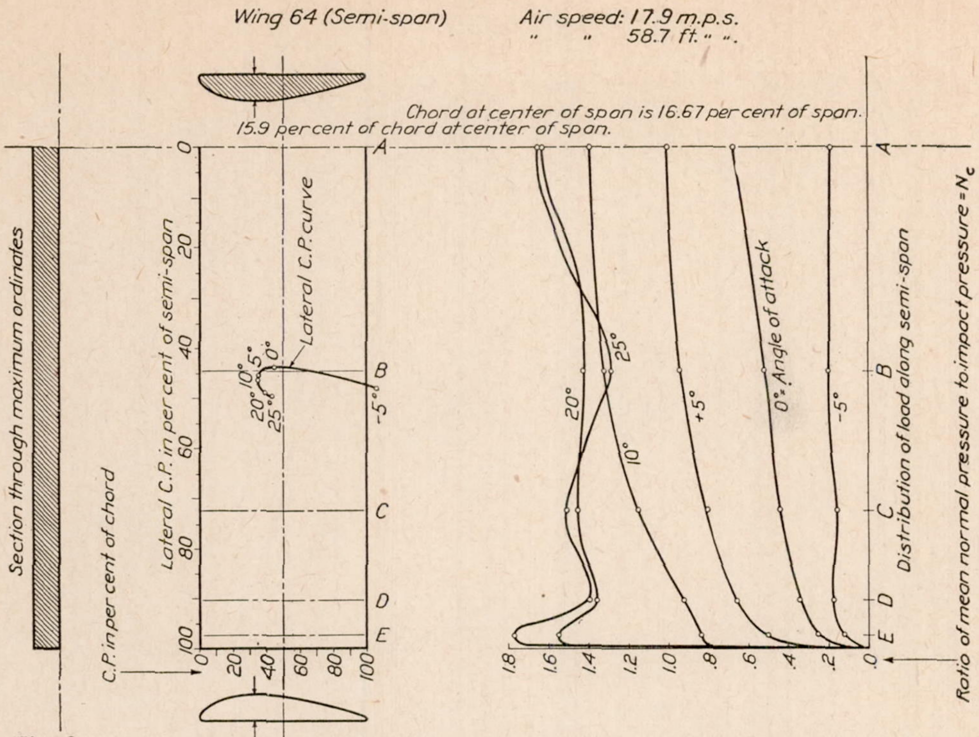

Fig. 13

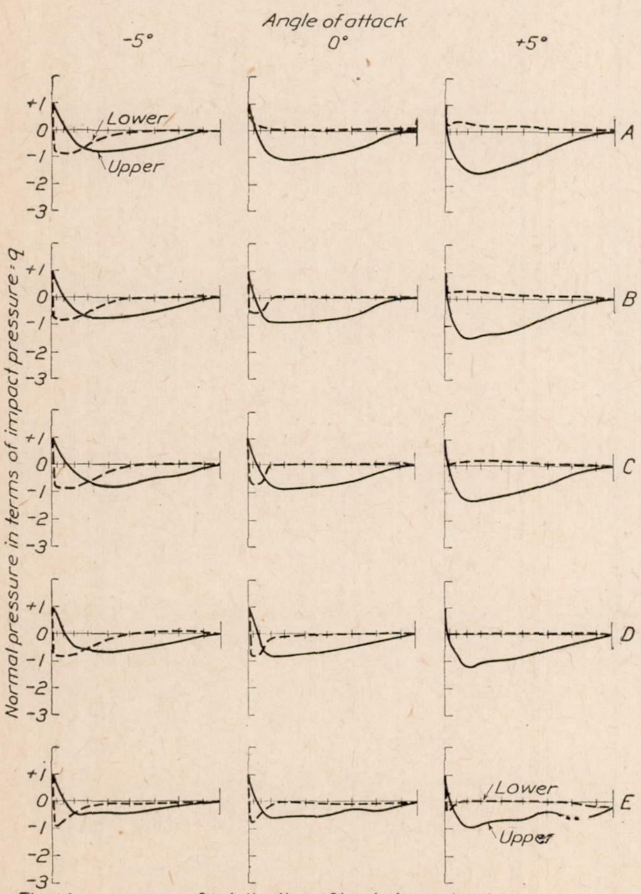

Fig. 14 Distribution of load along chord

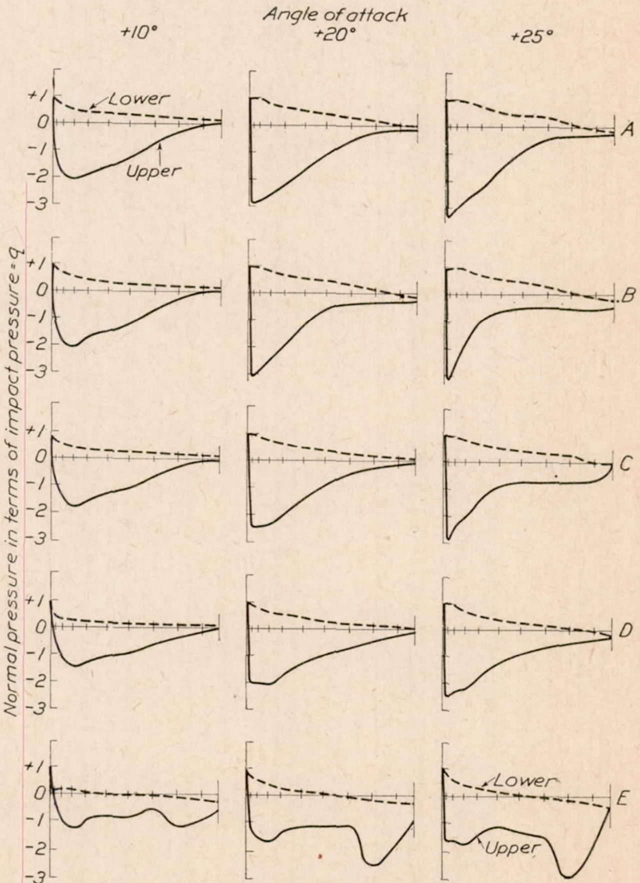

Fig. 14 Distribution of load along chord

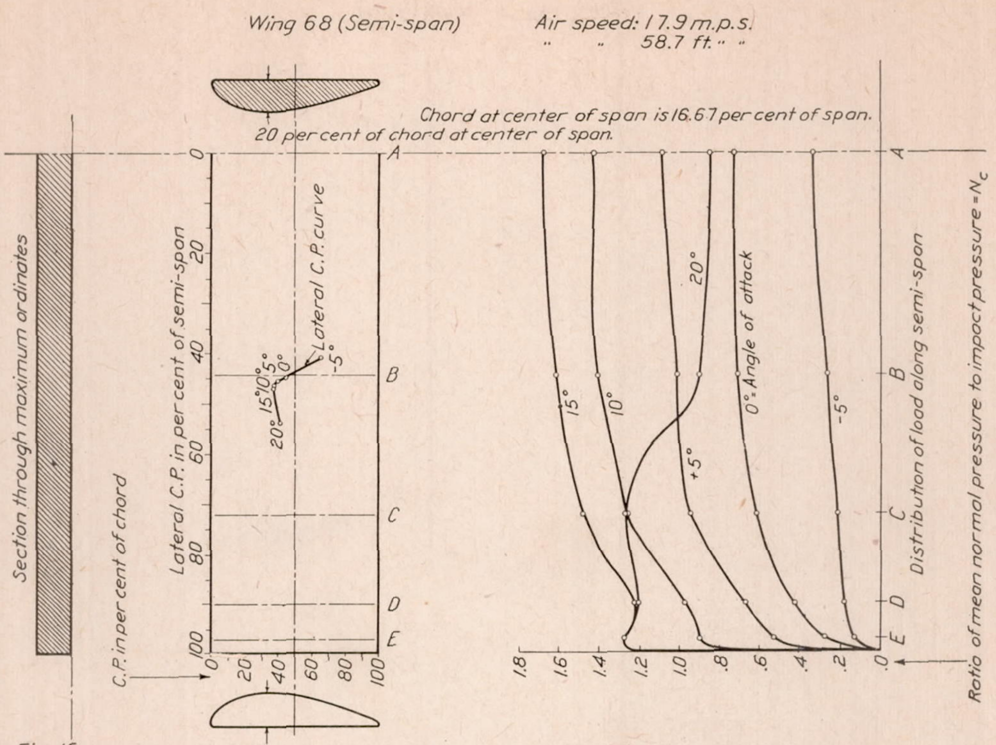
Wing 68 (Semi-span)
Air speed: 17.9 m.p.s.
" " 58.7 ft. " "
Chord at center of span is 16.67 per cent of span.
20 per cent of chord at center of span.
Section through maximum ordinates
C.P. in per cent of chord
Lateral C.P. in per cent of semi-span
Lateral C.P. curve
Distribution of load along semi-span
Ratio of mean normal pressure to impact pressure = N_c
0° Angle of attack
20 per cent of chord at tip.
Chord at tip is 16.67 per cent of span.

Fig. 15

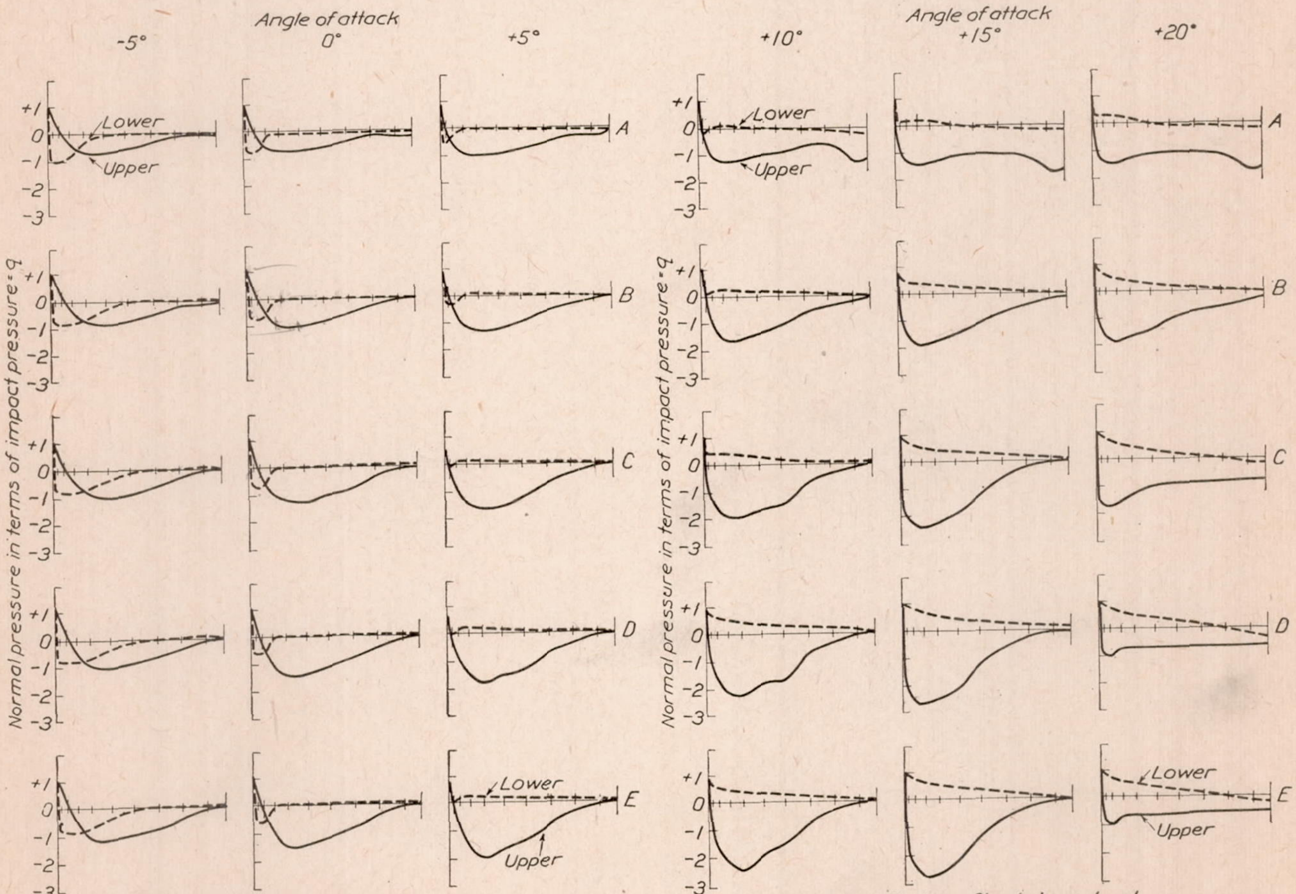
Angle of attack
-5°
0°
+5°
+10°
+15°
+20°
Lower
Upper
Normal pressure in terms of impact pressure = q
Distribution of load along chord

Fig. 16

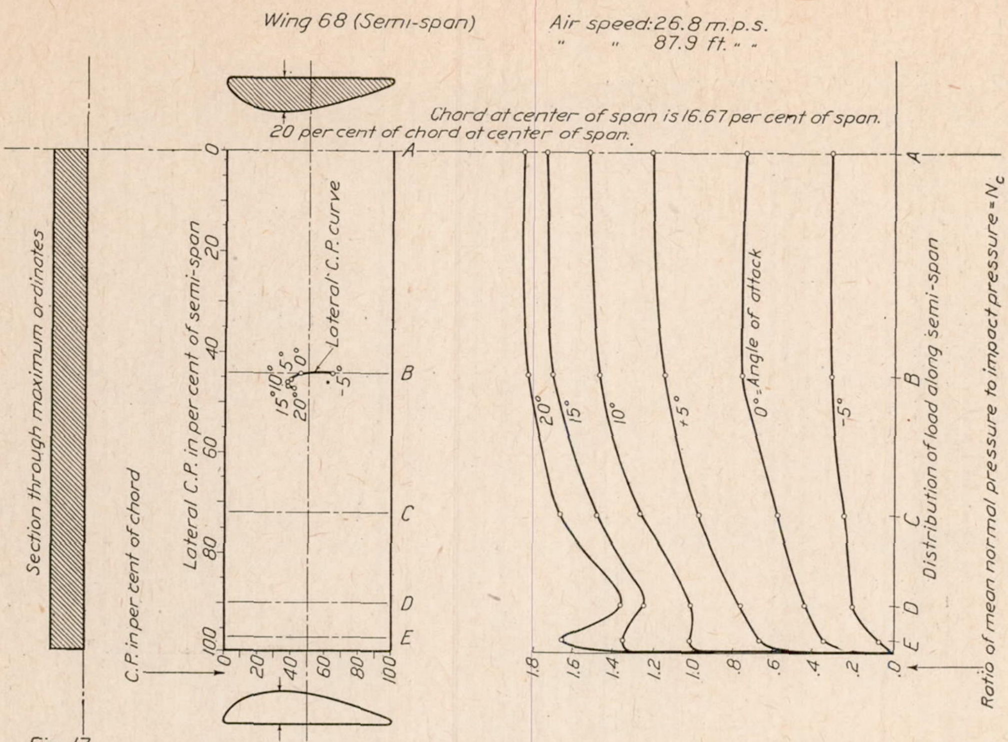

Fig. 17

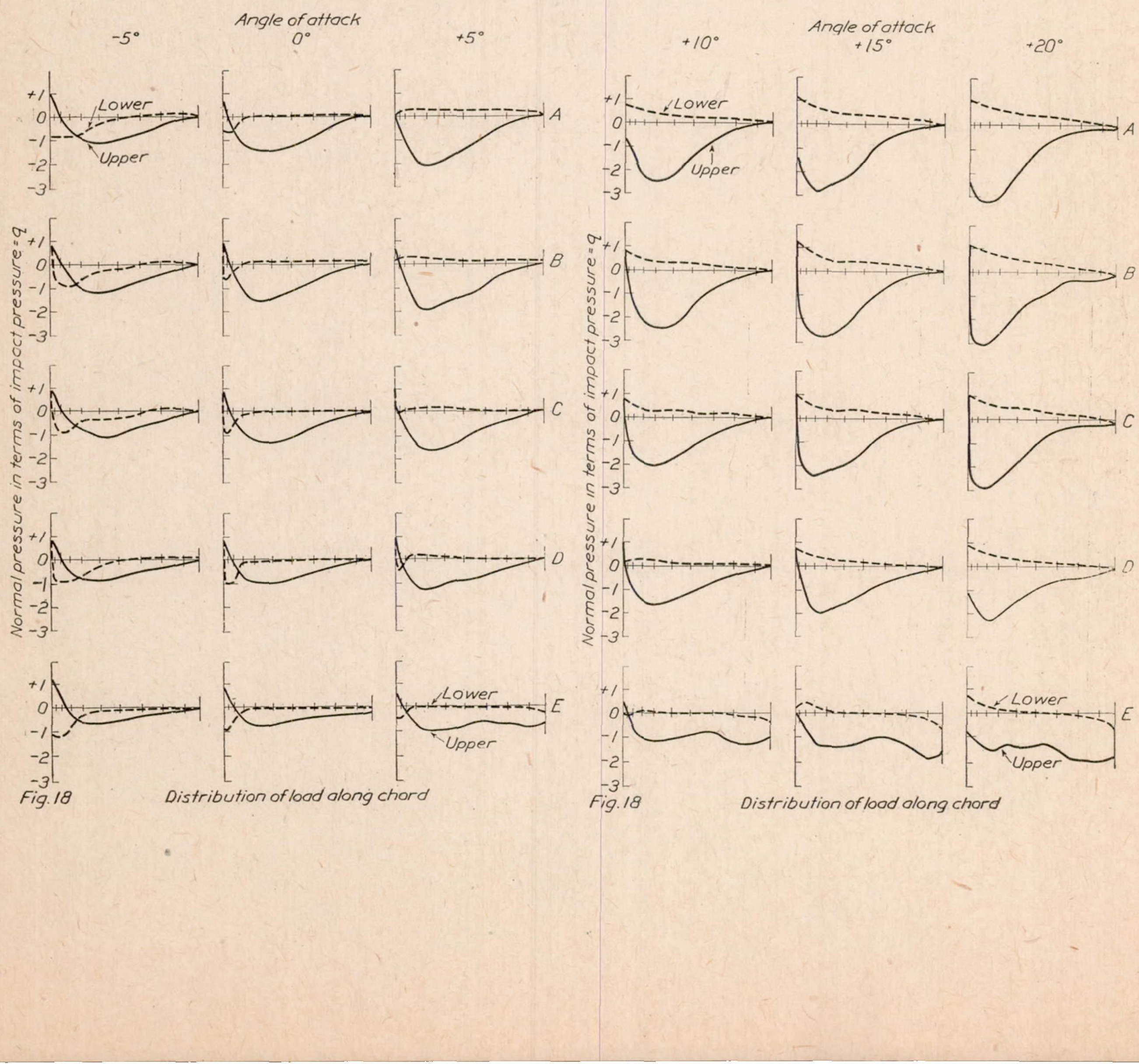

Fig. 18 Distribution of load along chord

Fig. 18 Distribution of load along chord

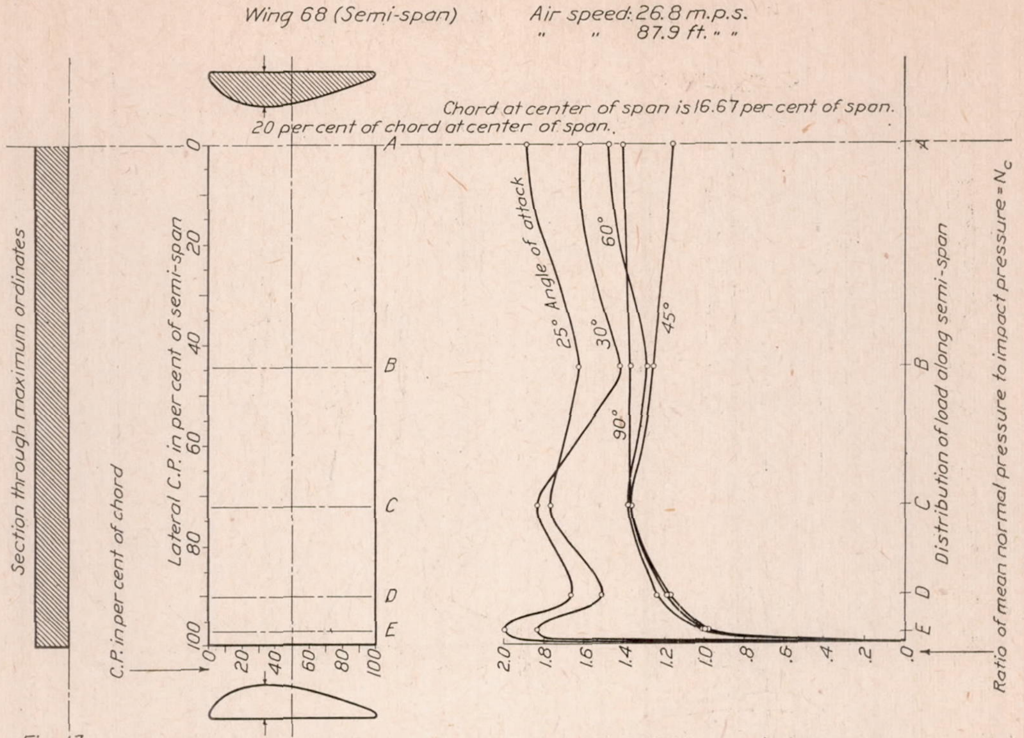

Fig. 17a

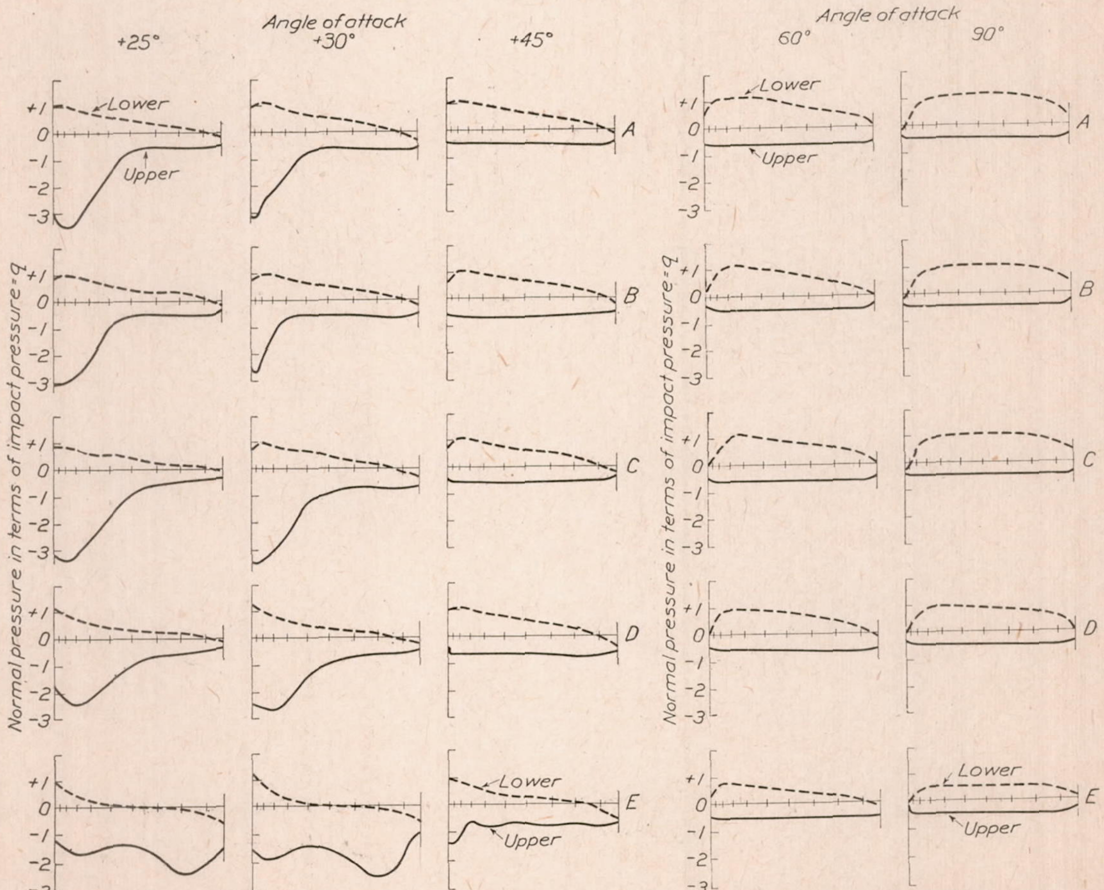

Fig. 19 Distribution of load along chord

Fig. 19 Distribution of load along chord

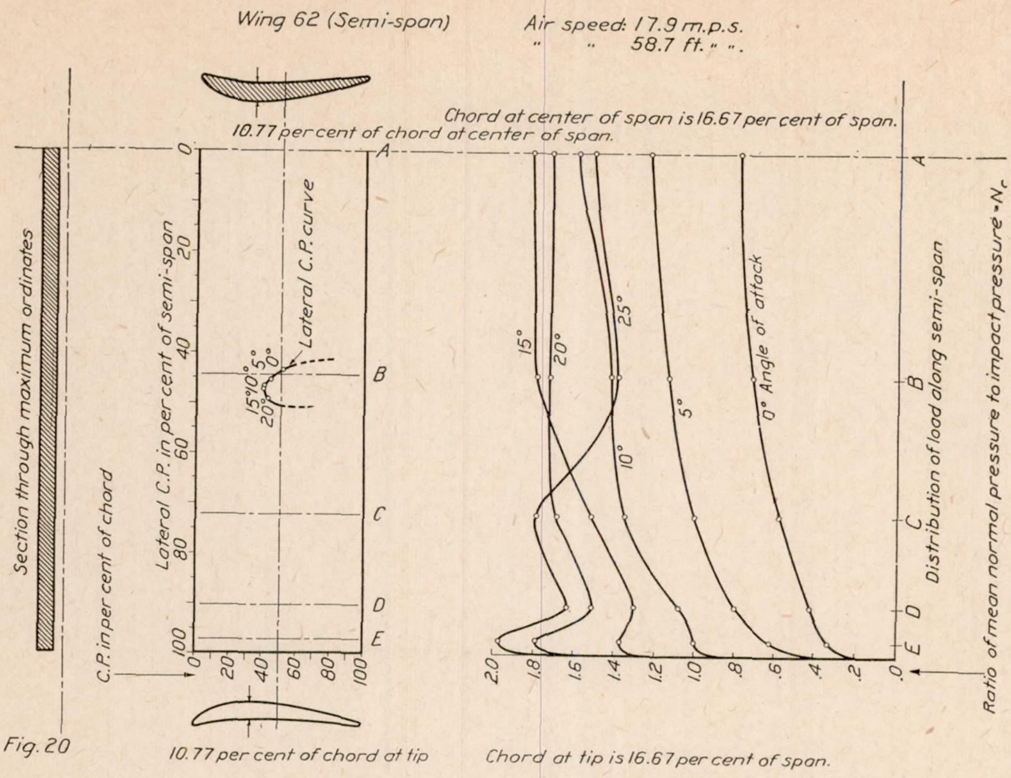
Wing 62 (Semi-span)
Air speed: 17.9 m.p.s.
" " 58.7 ft. " ".
Chord at center of span is 16.67 per cent of span.
10.77 per cent of chord at center of span.
Section through maximum ordinates
C.P. in per cent of chord
Lateral C.P. in per cent of semi-span
Lateral C.P. curve
Angle of attack
Distribution of load along semi-span
Ratio of mean normal pressure to impact pressure = N_c
10.77 per cent of chord at tip
Chord at tip is 16.67 per cent of span.

Fig. 20

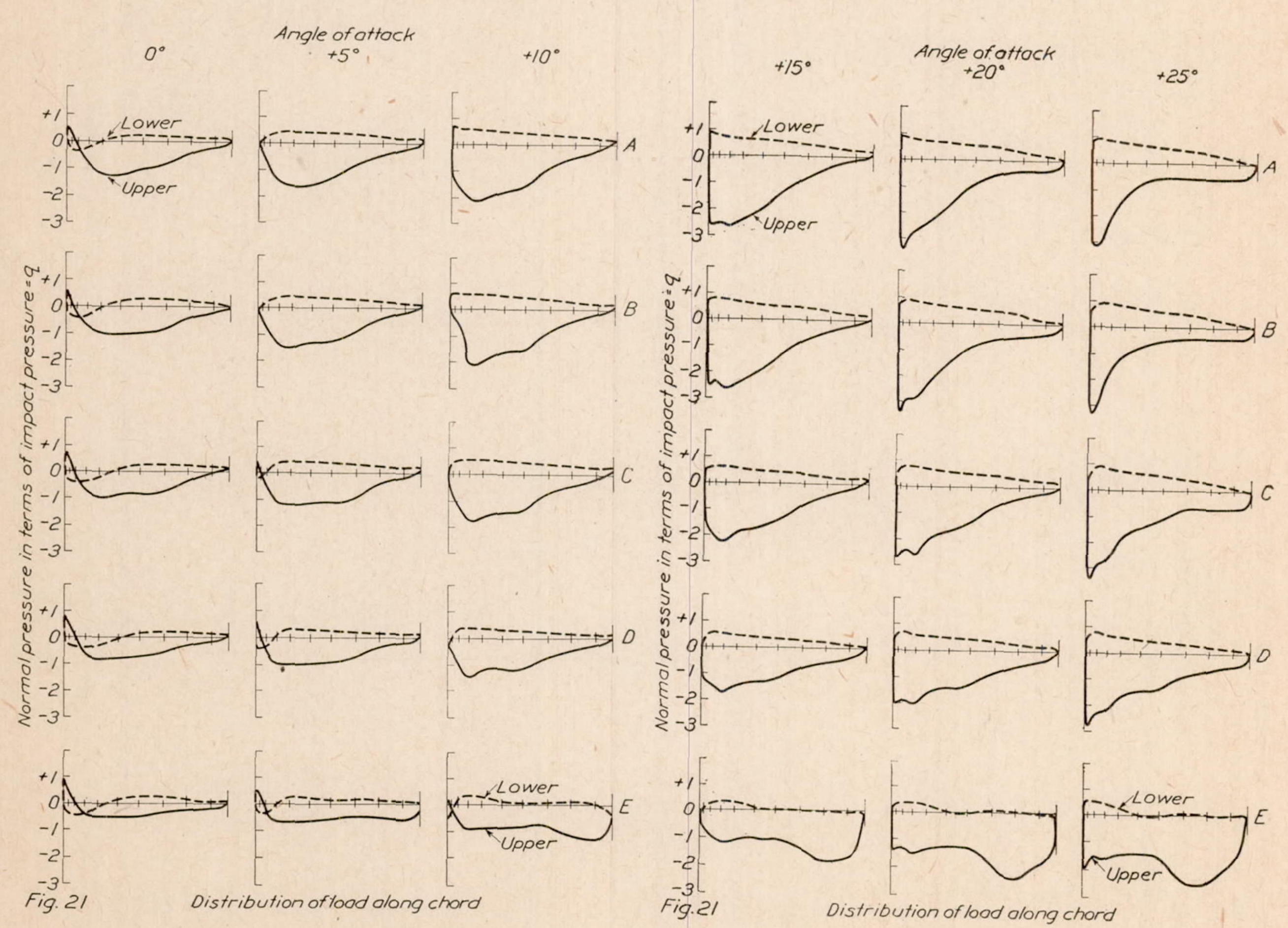
Angle of attack
0°
+5°
+10°
+15°
+20°
+25°
Lower
Upper
Normal pressure in terms of impact pressure = q
Distribution of load along chord

Fig. 21

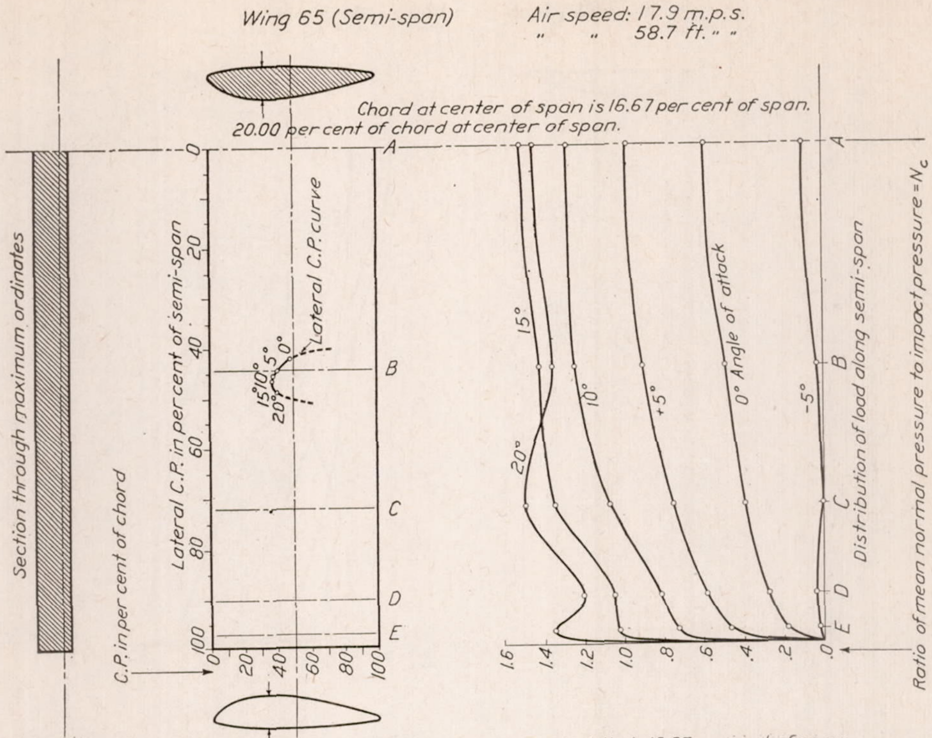

Fig. 22

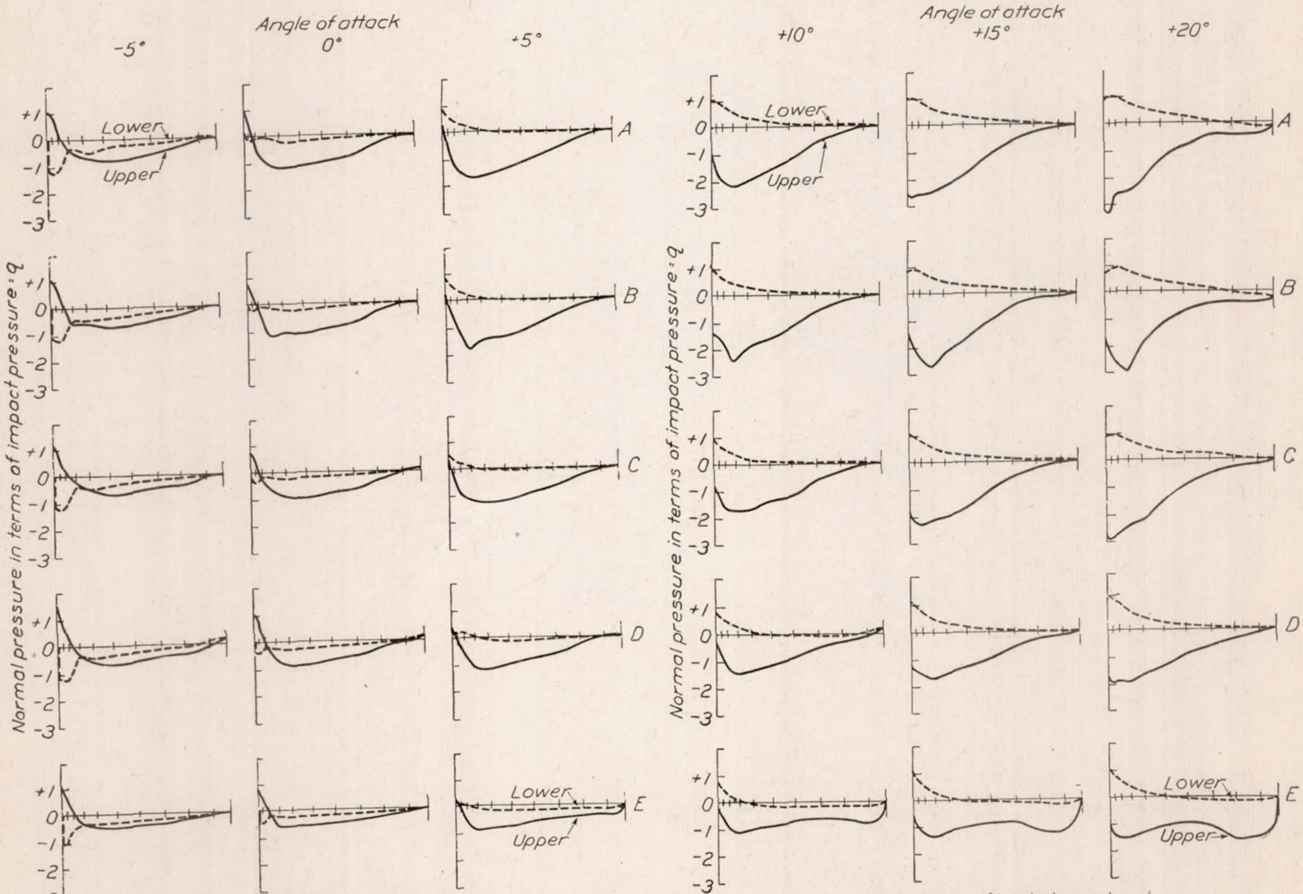

Fig 23 Distribution of load along chord

Fig. 23 Distribution of load along chord

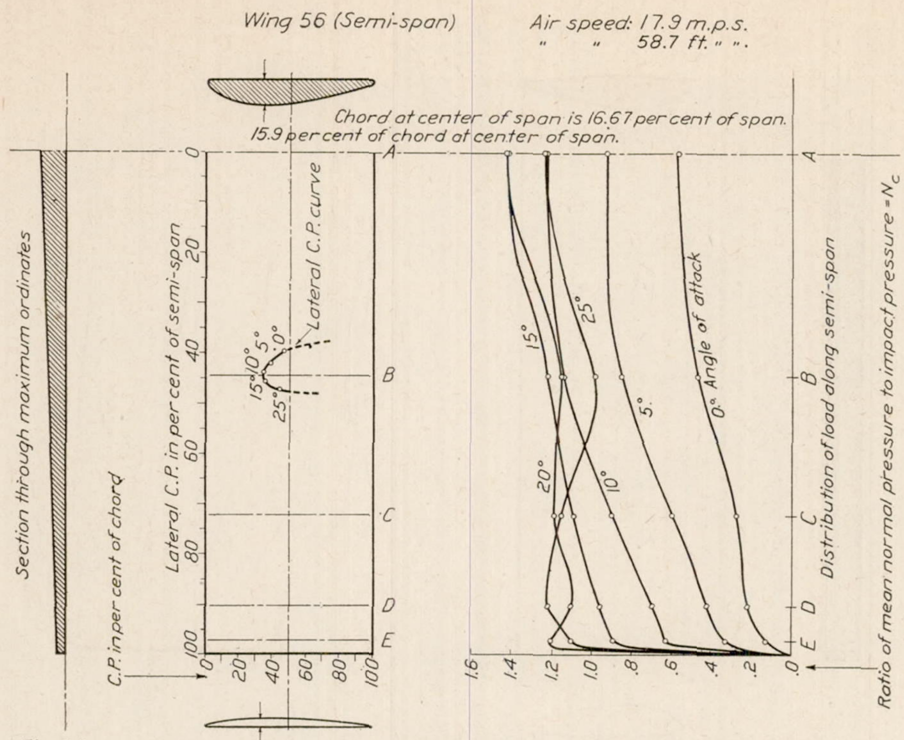

Fig. 24

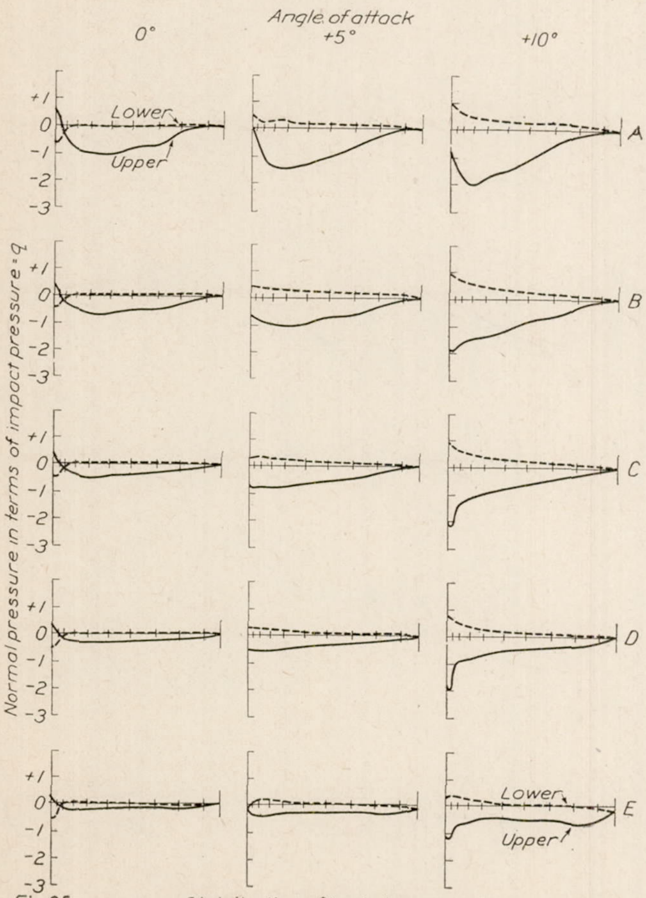

Fig. 25

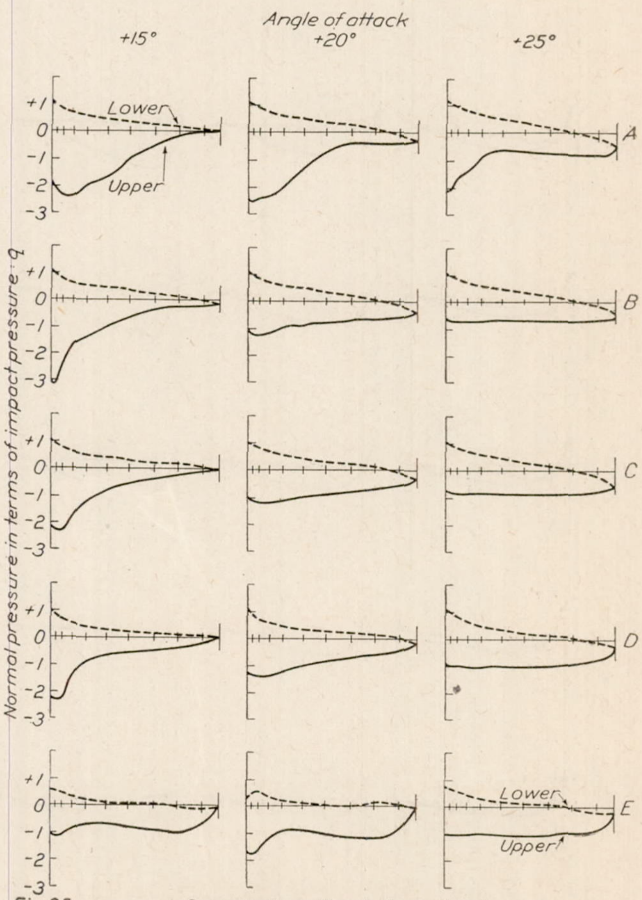

Fig. 25

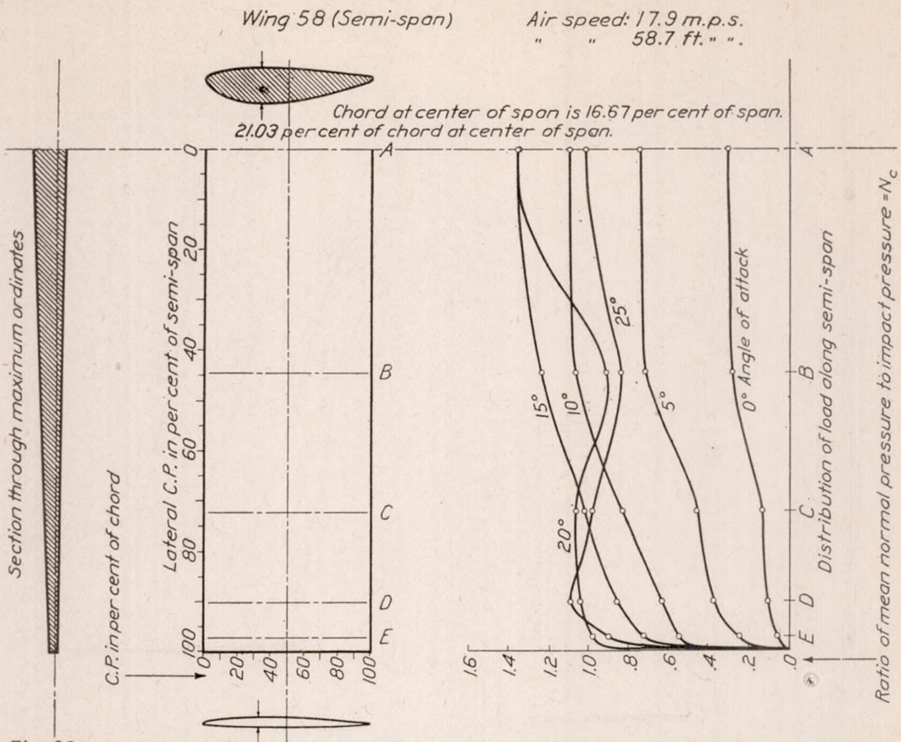
Wing 58 (Semi-span)
Air speed: 17.9 m.p.s.
" " 58.7 ft." ".
Chord at center of span is 16.67 per cent of span.
21.03 per cent of chord at center of span.
Section through maximum ordinates
Lateral C.P. in per cent of semi-span
C.P. in per cent of chord
Distribution of load along semi-span
Ratio of mean normal pressure to impact pressure = N_c
0° Angle of attack
5°
10°
15°
20°
25°
A
B
C
D
E
5.25 per cent of chord at tip.
Chord at tip is 16.67 per cent of span.

Fig. 26

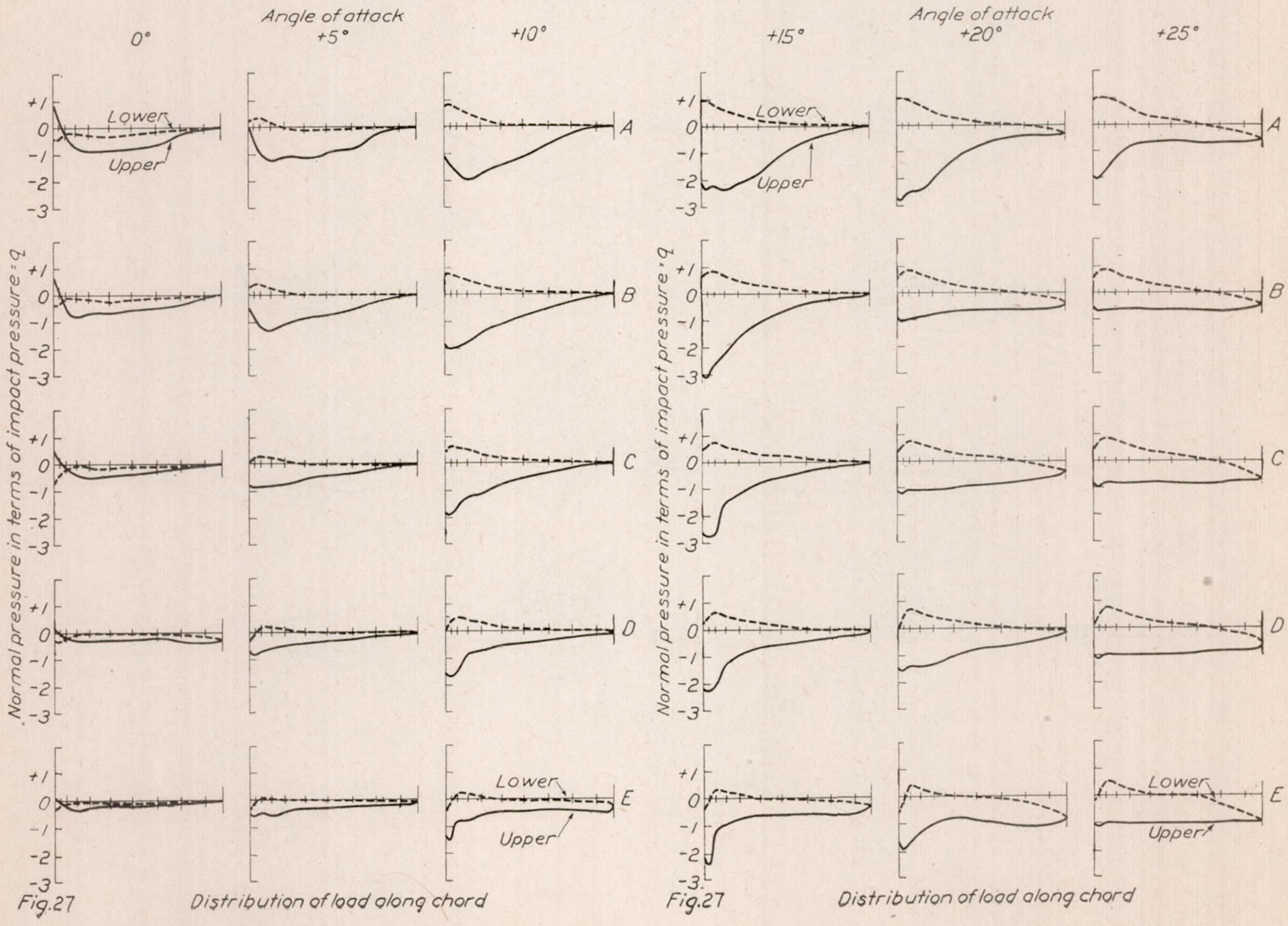
Angle of attack
0°
+5°
+10°
+15°
+20°
+25°
Lower
Upper
Normal pressure in terms of impact pressure = q
A
B
C
D
E
Distribution of load along chord

Fig. 27

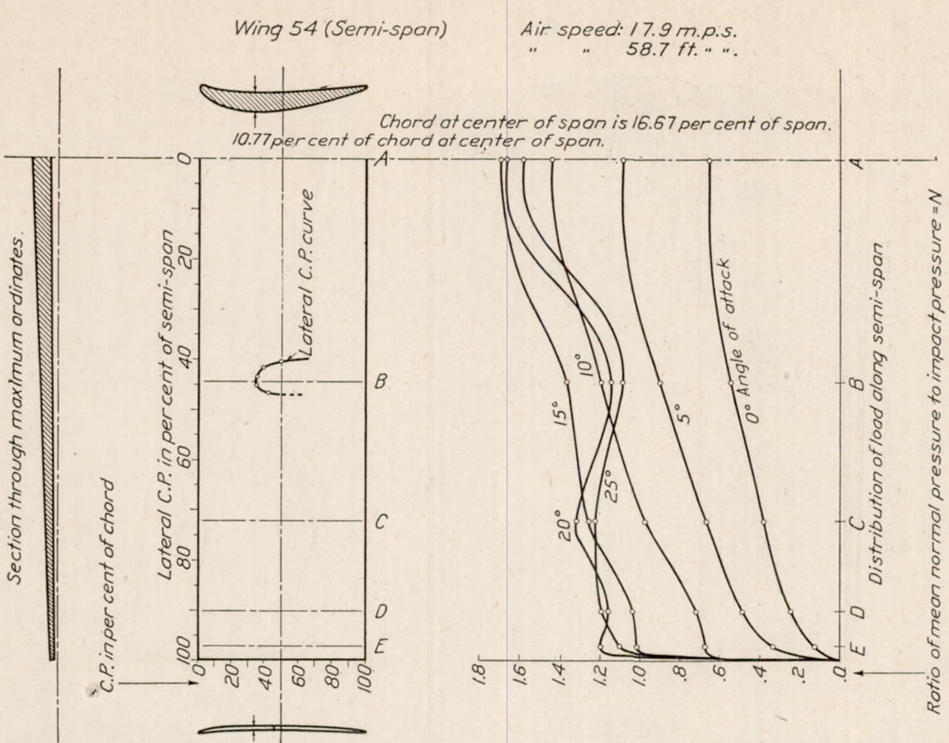

Fig. 28

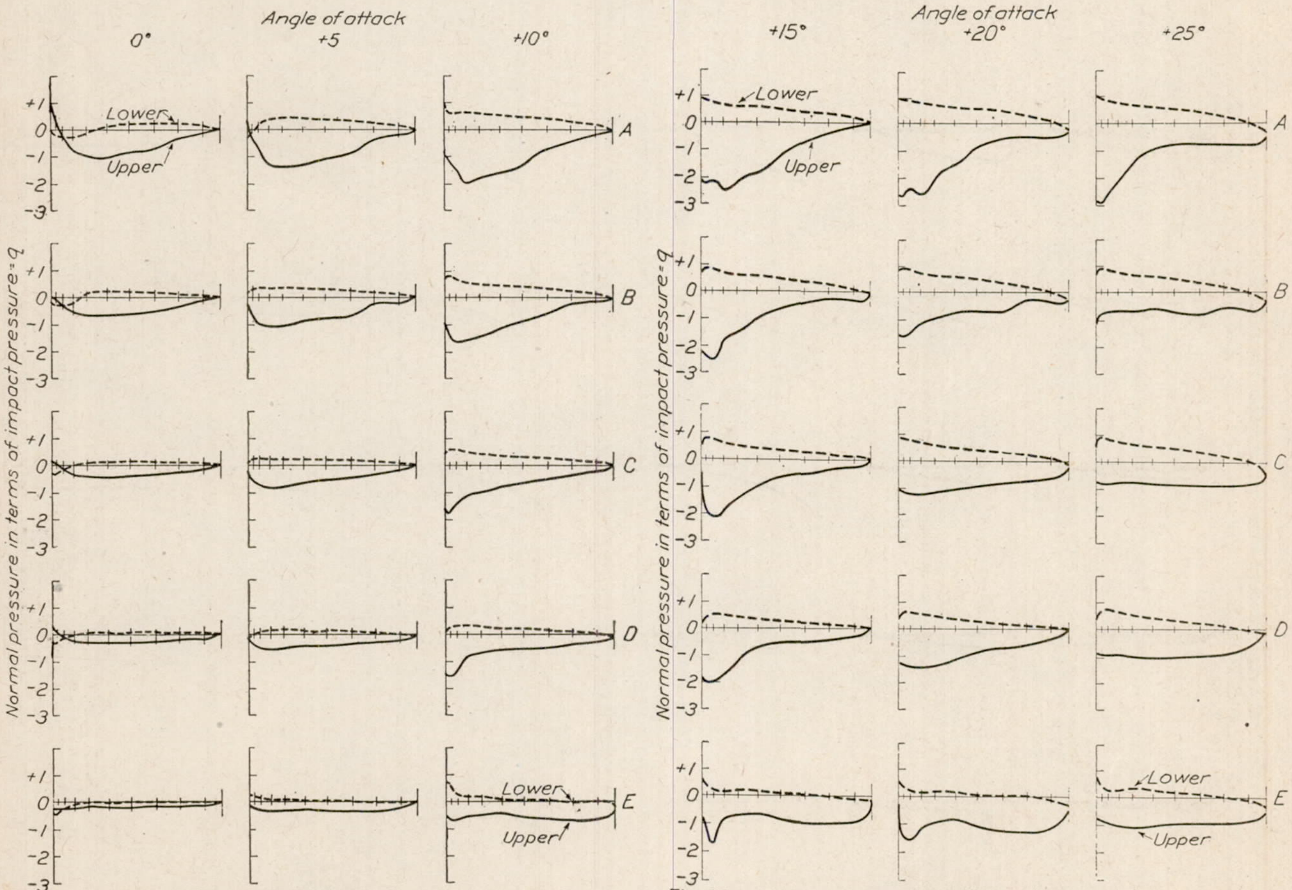

Fig. 29 Distribution of load along chord

Fig. 29 Distribution of load along chord

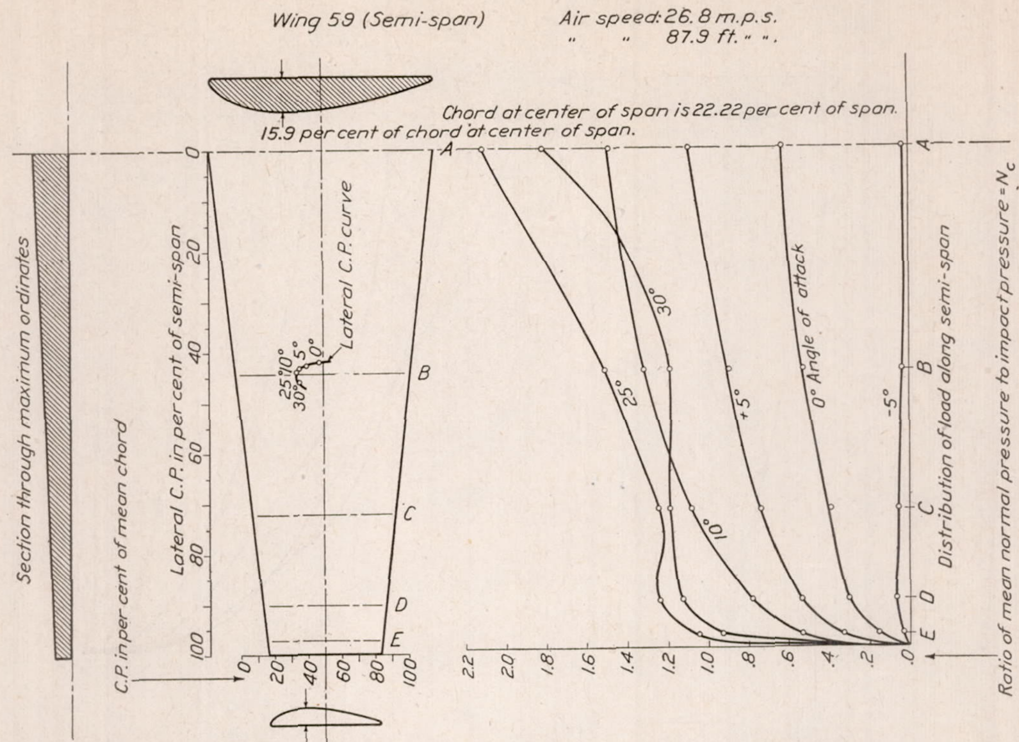
Wing 59 (Semi-span)
Air speed: 26.8 m.p.s.
" " 87.9 ft. " ".
Chord at center of span is 22.22 per cent of span.
15.9 per cent of chord at center of span.
Section through maximum ordinates
C.P. in per cent of mean chord
Lateral C.P. in per cent of semi-span
Lateral C.P. curve
Angle of attack
Distribution of load along semi-span
Ratio of mean normal pressure to impact pressure = N_c
15.9 per cent of chord at tip.
Chord at tip is 11.11 per cent of span.

Fig. 30

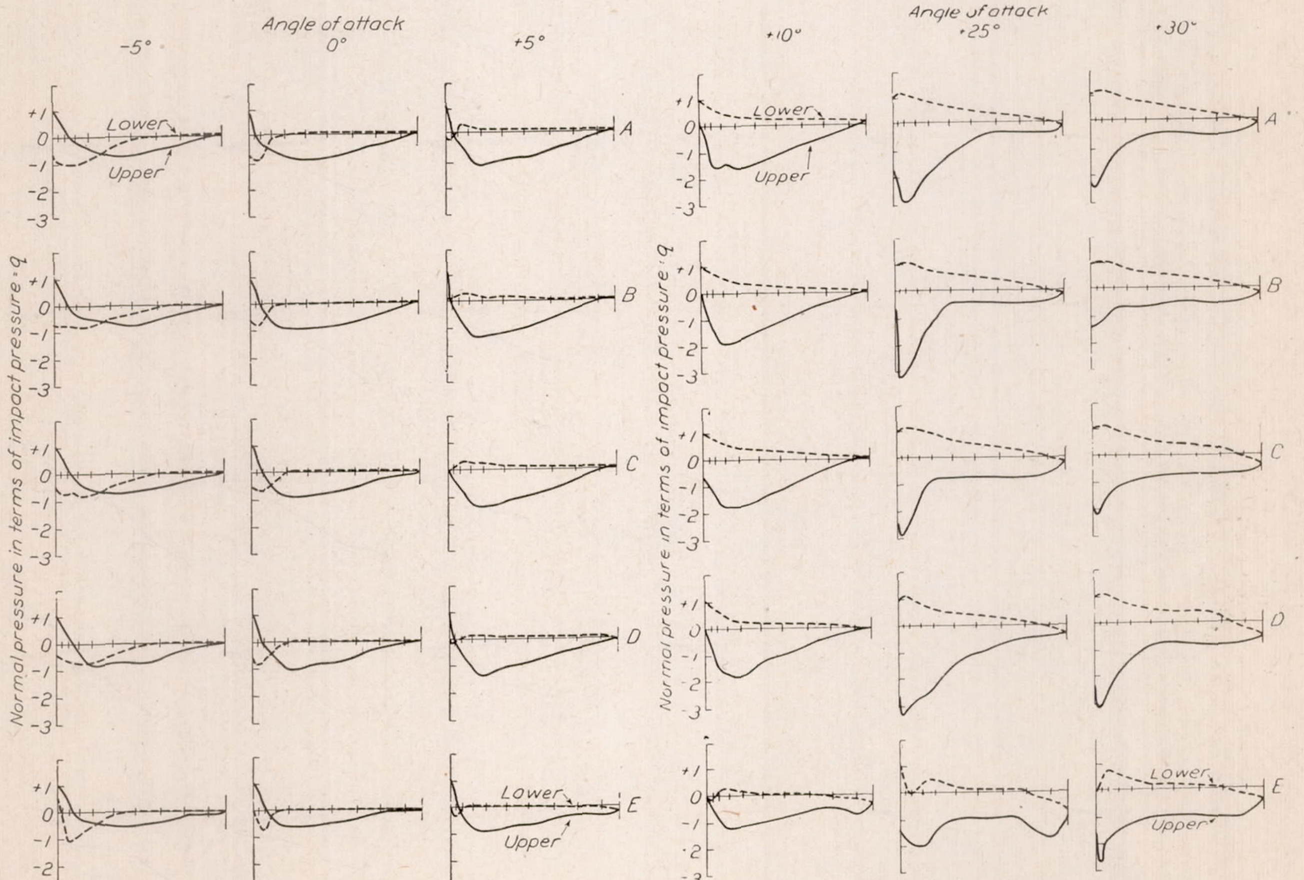
Angle of attack
-5°
0°
+5°
+10°
+25°
+30°
Lower
Upper
Normal pressure in terms of impact pressure · q
Distribution of load along chord

Fig. 31

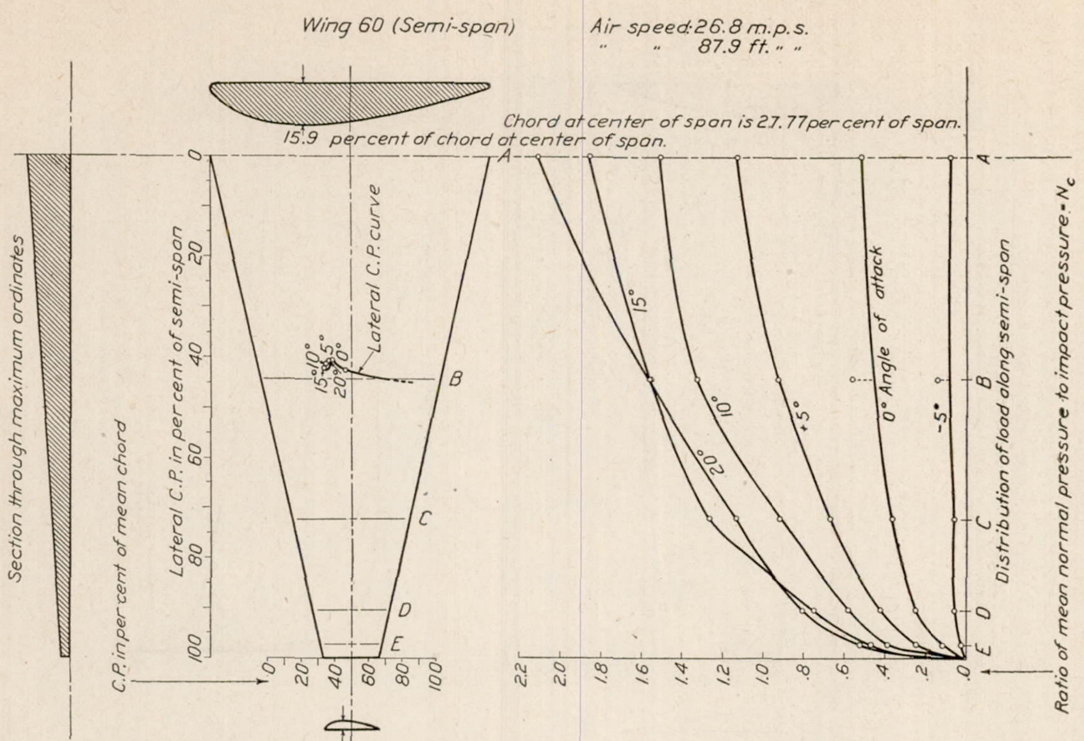

Fig. 32

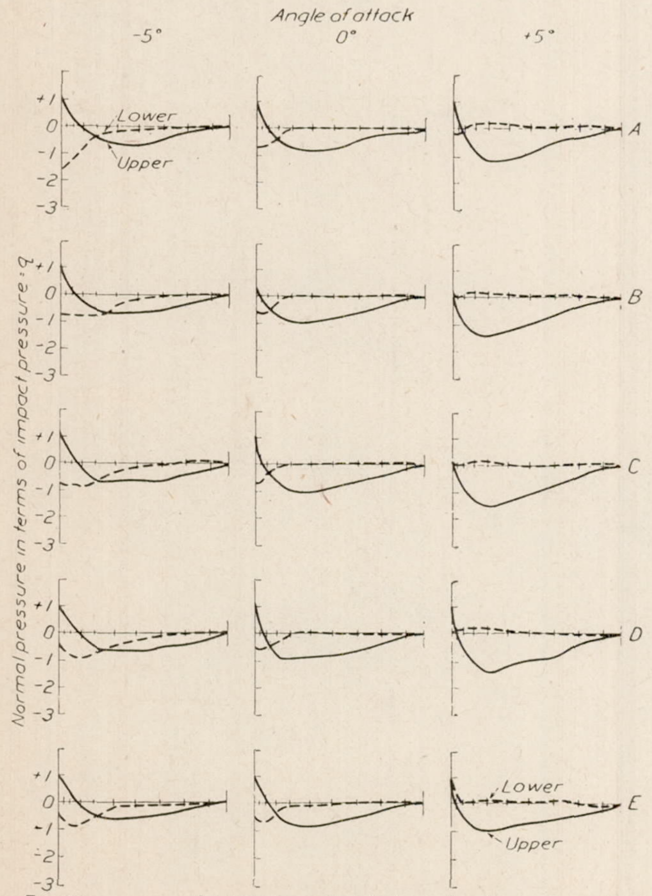

Fig 33 Distribution of load along chord

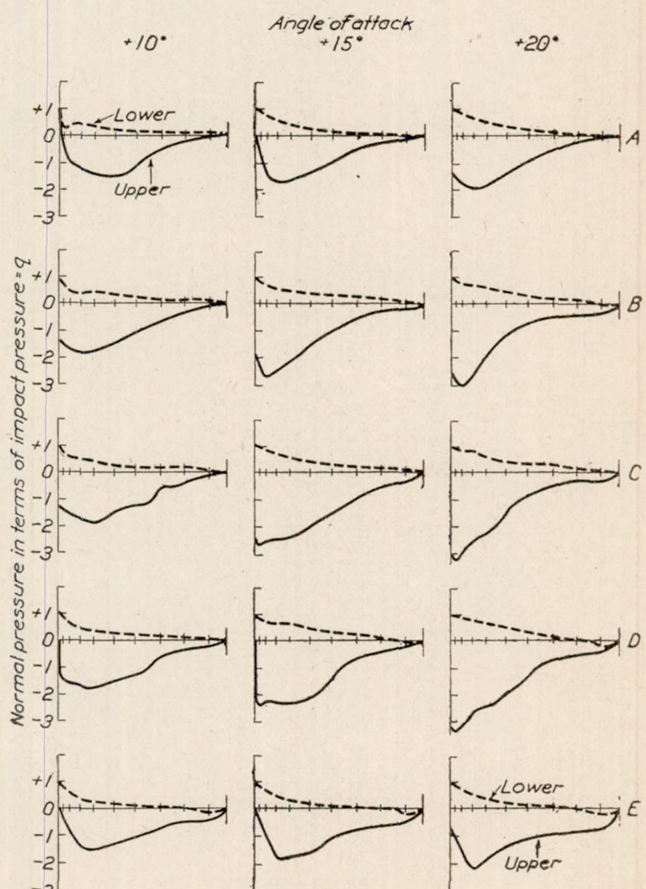

Fig. 33 Distribution of load along chord

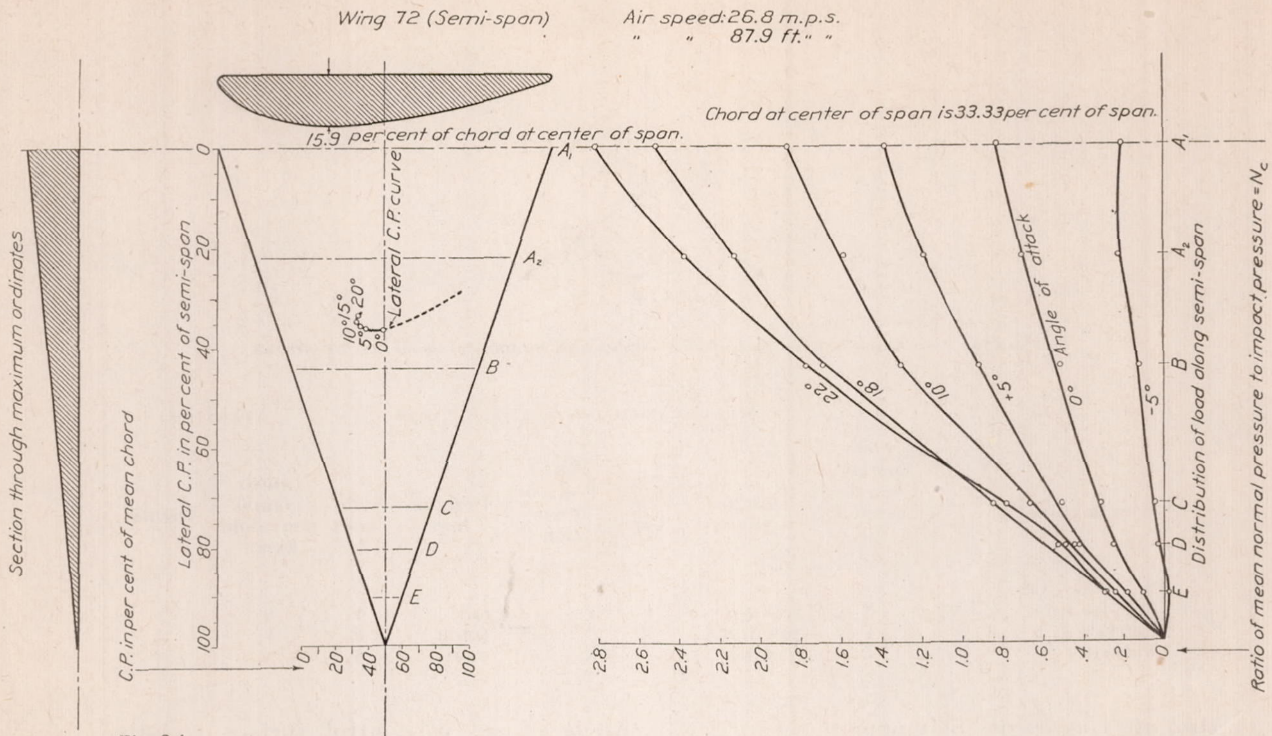

Fig. 34

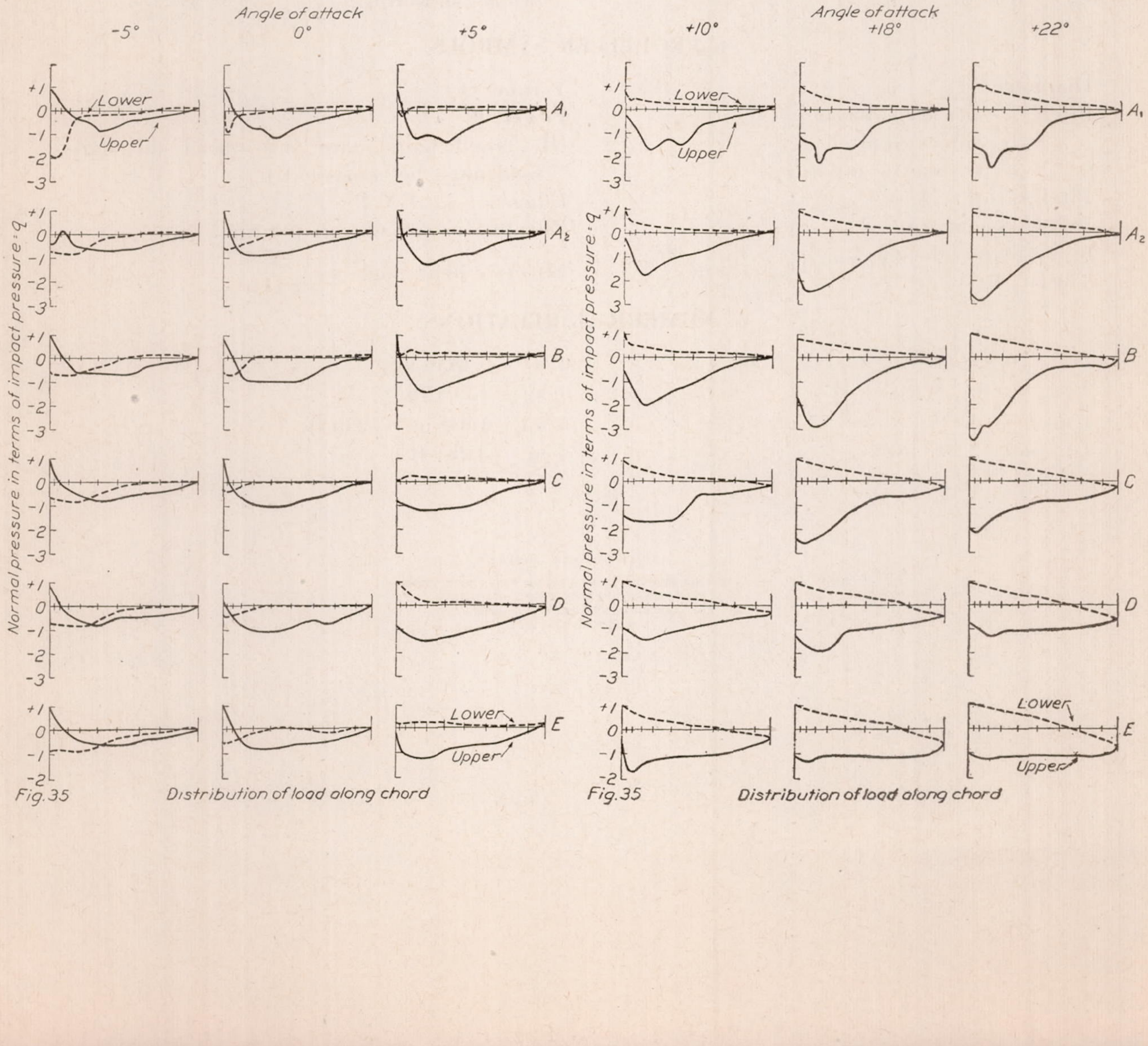

Fig. 35 Distribution of load along chord

Fig. 35 Distribution of load along chord

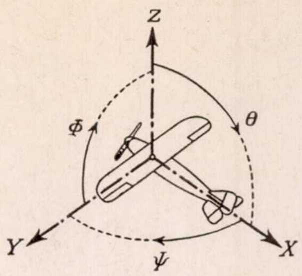

Positive directions of axes and angles (forces and moments) as shown by arrows.

Axis.		Force (parallel to axis) symbol.	Moment about axis.			Angle.		Velocities.	
Designation.	Symbol.		Designation.	Symbol.	Positive direction.	Designation.	Symbol.	Linear (component along axis).	Angular.
Longitudinal....	X	X	rolling.....	L	Y⟶Z	roll......	Φ	u	p
Lateral..........	Y	Y	pitching...	M	Z⟶X	pitch....	θ	v	q
Normal..........	Z	Z	yawing.....	N	X⟶Y	yaw.....	Ψ	w	r

Absolute coefficients of moment

$C_l = \frac{L}{q\,b\,S}$, $C_m = \frac{M}{q\,c\,S}$, $C_n = \frac{N}{q\,f\,S}$

Angle of set of control surface (relative to neutral position), δ. (Indicate surface by proper subscript.)

4. PROPELLER SYMBOLS.

Diameter, D

Pitch (a) Aerodynamic pitch, p_a

(b) Effective pitch, p_e

(c) Geometric pitch, p_g

Pitch ratio, p/D

Inflow velocity, V′

Slip-stream velocity, V_s

Thrust, T

Torque, Q

Power, P

(If "coefficients" are introduced all units used must be consistent.)

Efficiency $\eta = T\,V/P$

Revolutions per sec., n; per min., N.

Effective helix angle $\Phi = \frac{V}{\pi D n}$

5. NUMERICAL RELATIONS.

1 HP = 76 kg. m/sec. = 550 lb. ft/sec.

1 kg. m/sec. = 0.01315 HP

1 mi/hr. = 0.4470 m/sec.

1 m/sec. = 2.237 mi/hr.

1 lb. = 0.4536 kg.

1 kg. = 2.204 lb.

1 mi. = 1609 m. = 5280 ft.

1 m. = 3.281 ft.

ADDITIONAL COPIES
OF THIS PUBLICATION MAY BE PROCURED FROM
THE SUPERINTENDENT OF DOCUMENTS
GOVERNMENT PRINTING OFFICE
WASHINGTON, D. C.
AT
5 CENTS PER COPY
∇